A COMPARISON OF CONVENTIONAL HEATING TECHNIQUES AND MICROWAVE IRRADIATION FOR THE DESORPTION OF LITHIUM BOROHYDRIDE AND LITHIUM BOROHYDRIDE COMPOSITES

BY JAMES FARMER

A thesis submitted to

The University of Birmingham

for the degree of

MASTER OF RESEARCH

Department of Metallurgy and Materials

School of Engineering

The University of Birmingham

August 2009

Abstract

The desorption of lithium borohydride and lithium borohyride composites was examined using both conventional heating techniques and microwave irradiation.

$LiBH_4$ was milled with TiH_2 in various molar ratios in an argon atmosphere using both roller and planetary mill techniques. Thermo-gravimetric analysis and differential scanning calorimetry determined the desorption characteristics of the as received and milled materials. Scanning electron microscopy was used to examine the particle size of the materials before heating.

A temperature programmed desorption (TPD) rig and a custom built microwave rig were both connected to the same gas sorption system which was pressurised with hydrogen and could be operated with each system independently. A comparison in desorption characteristics was made between conventional TPD heating techniques and microwave irradiation for the as received and milled materials; mass flow controllers were able to measure the amount of hydrogen desorbed in both cases. X-ray diffraction was conducted on the samples before and after heating in the TPD rig.

TiH_2 was found to kinetically destabilise the desorption of $LiBH_4$ in all techniques. Microwave induced desorption produced faster heating rates than were exhibited with conventional heating techniques using less energy, with similar amounts of hydrogen gas being desorbed in a much shorter time period.

Table of Contents

List of Illustrations of Tables

Figure

Table

1. Introduction

An estimated 6.7 billion people inhabit our world today [1]; the rapid increase in population has intensified the requirement for a reliable and abundant energy source in order to cope with the escalating power demands of our society.

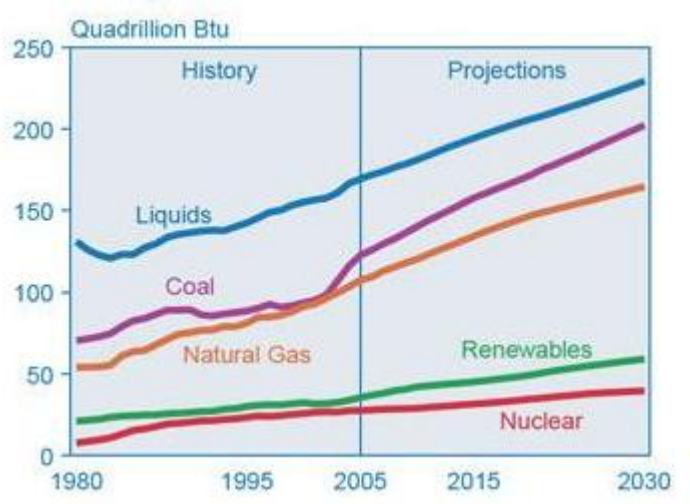

Figure 1 – EIA World Marketed Energy Use by Fuel Type, 1980-2030 [2]

Figure 1 demonstrates the huge dependence currently placed on energy production from fossil fuels, with only a very small proportion being attributed to renewable energies.

Not only are fossil fuels highly polluting, producing large amounts of carbon dioxide and other greenhouse gases, they also have a very limited life span with reserves expected to run out within the next century. As of 2008, the U.S Energy Information Administration predicts natural gas reserves to be exhausted within 63 years [3]. The irreversible damage these fossil fuels are causing includes signs of the polar ice caps melting and significant changes in climate. Energy security is also an important issue, particularly for the UK which has limited renewable energy sources and has been forced to import increasing amounts of oil from politically sensitive areas such the Middle East.

Solutions must be found to protect the energy needs of the country: the increased use of renewable energy such as wind, hydroelectric, solar and tidal power offers a partial solution. These types of renewable sources come with large initial outlays, although they do provide a clean and abundant energy source that can be employed throughout the country. However, these sources of power suffer from poor reliability and intermittency, since large amounts of energy are generated only when the weather is suitable. Renewable energy sources are also unable to match power demands at peak periods that a conventional coal or natural gas power station could.

It may be possible for these problems to be partially solved with the introduction of a hydrogen economy which offers a realistic energy storage solution. There are various advantages for the use of hydrogen as a fuel in both static and mobile applications; hydrogen has the highest energy density per unit mass of any fuel and can be produced from numerous sources such as electrolysis of water and steam reforming of natural gas. For a PEM fuel cell, the only resulting by-product is water which can be electrolysed to produce hydrogen and oxygen once again. Unlike conventional fossil fuel powered engines, a fuel cell is able to operate at much higher efficiencies of up to 65 % - 70 % in mobile and static applications, compared with values in the order of 40 % for internal combustion engines. Therefore hydrogen storage offers a clean, non polluting energy system, it is important to examine possible storage techniques and understand the barriers which presently prevent its introduction.

2. Literature Review

2.1 Introduction to Solid State Storage

There are various methods of storing hydrogen shown by figure 2; these include gaseous, liquid and solid state storage. Although hydrogen offers a favourable amount of energy per unit mass when compared with other fuels such as petroleum, when stored in gaseous form it exhibits a poor amount of energy per unit volume. This makes mobile applications for hydrogen increasing difficult, due to lack of storage space for the fuel.

Figure 2 – Volumetric requirements for 4kg of hydrogen stored in different ways [4]

Liquefied hydrogen offers a more favourable amount of energy per unit volume compared to compressed hydrogen gas. As shown in figure 2, liquid hydrogen fuel can be stored in almost half the volume required for gaseous storage at 200 bar pressure. 4kg of liquefied hydrogen can be stored in 57 litres, compared with 110 litres when stored as a gas. However, to reach and maintain the temperatures required for liquefaction requires a large amount of energy meaning that any advantage gained by

a smaller volume of fuel is cancelled out in energy losses. For mobile applications, the spatial requirements of large tank insulations to minimise liquid boil-off also become a serious problem and make this type of storage unfavourable.

This problem can be overcome by storing the hydrogen in a complex hydride such as Mg_2FeH_6 which allows for the same 4kg of hydrogen to be stored within only 26 litres, using less than a quarter of the volume required for gaseous storage. The major challenge with solid-state hydrogen materials arises from trying to attain the maximum gravimetric and volumetric H_2 density possible, while maintaining a low H_2 decomposition temperature. As shown in figure 3, Mg_2FeH_6 allows a favourable 5.5 wt% to be stored within the material, however a decomposition temperature of 620 K is a problem.

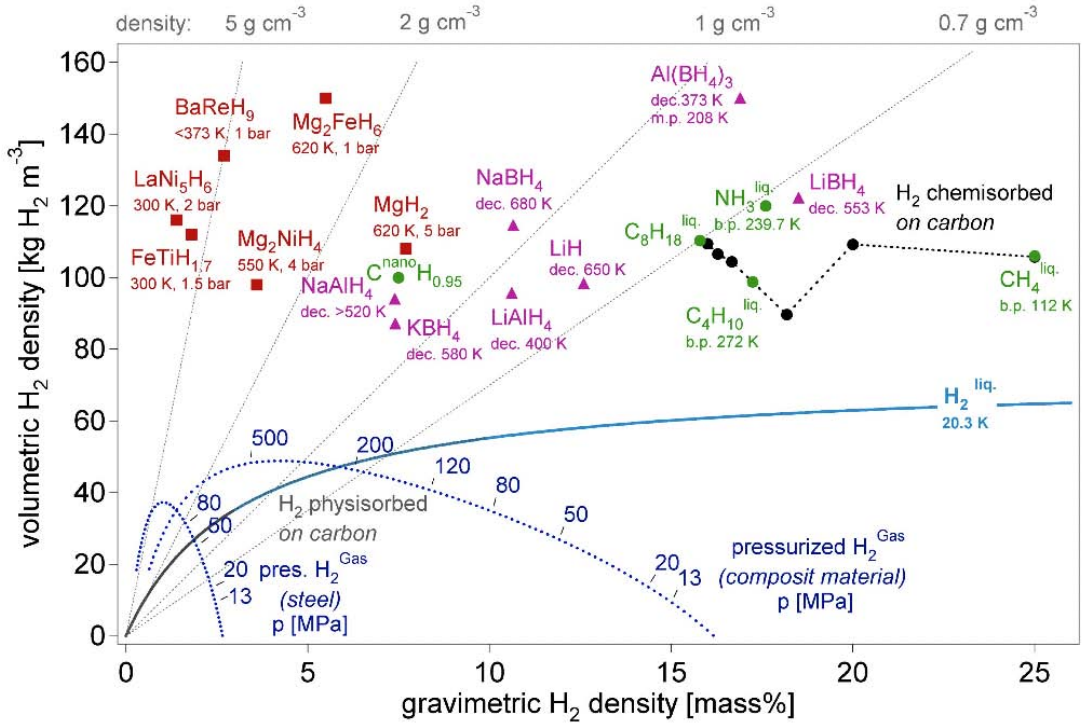

Figure 3 - Volumetric density against gravimetric density for a range of solid state hydrogen storage materials [5]

Materials such as $FeTiH_{1.7}$, $BaReH_9$ and Mg_2FeH_6 contain heavy transition metal elements which greatly reduce the gravimetric H_2 density reducing their suitability for hydrogen storage, particularly in mobile storage where heavy cylinders would significantly reduce performance. The light metal hydrides are more favourable for hydrogen storage since they contain elements with far smaller atomic masses in the alkali and alkaline earth metal series: MgH_2 and LiH offer significant increases in gravimetric H_2 density.

The US Department of Energy (DOE) has set targets for both gravimetric and volumetric capacities for on-board hydrogen storage systems, detailed in table 1.

Storage Parameter	Units	2007	2010	2015
Gravimetric	wt%	4.5	6	9
Volumetric	kg H_2 / m^3	36	45	81

Table 1 – US DOE on-board hydrogen storage system performance targets [6]

However, there are many other factors to consider in respect to the viability of a hydrogen solid state storage material, such as:

- Suitable temperature and pressure range for operation of the system
- Reversibility of the system and resistance against degradation after repeated cycling
- Good reaction kinetics in both dehydrogenation and recombination processes
- High purity of hydrogen produced to prevent poisoning of PEM fuel cells
- Economically viable

Recently the characteristics of borohydrides have been examined, $M(BH_4)$ where M = K, Na, Li. These materials enable a large weight percentage of hydrogen to be stored

within the substance since the boron atom allows 4 hydrogen atoms to bond to it creating a $[BH_4]^-$ anion, this then forms a weak ionic bond to the alkali metal. These borohydrides partly satisfy the DOE storage targets for 2010; $LiBH_4$ offers the largest storage potential with 18.5 wt% gravimetric storage and 121 kg / m^3 volumetric storage. The suitability of these materials with respect to temperature and pressure range of operation, reversibility and reaction kinetics will now be examined.

2.2 Borohydrides as solid state storage materials

2.2.1 $LiBH_4$ Properties

Borohydrides have attracted much attention in the hydrogen storage field; materials such as KBH_4, $NaBH_4$ and $LiBH_4$ offer a large wt% of hydrogen to be stored within the material, 7.4 %, 10.6 % and 18.4 % respectively. Currently $LiBH_4$ is the prominent material; its volumetric density is slightly smaller than that of other hydrogen storage materials such as MgH_2 or KBH_4, but unlike these materials, $LiBH_4$ offers a large increase in gravimetric H_2 density. This is due to the Li atom having a small atomic mass in comparison to the other metals bonded to the borohydride anion such as Na or K. [7]

2.2.2 Conventional Heating

To be a useful hydrogen store in both mobile and static applications, the hydrogen in the solid state store must be able to be liberated easily allowing for the fuel to be combusted. $LiBH_4$ is particularly stable and exhibits poor hydrogen desorption kinetics requiring high temperatures to desorb any hydrogen.

When $LiBH_4$ is heated, a structural change is observed at 120°C and a small hydrogen desorption occurs, the orthorhombic structure observed at ambient temperatures changes to a hexagonal structure, and a fusion reaction then occurs at 280°C. A slightly larger percentage of hydrogen is desorbed when the material reaches 320°C and the third most prominent hydrogen peak occurs between approximately 450 - 500°C. These energy requirements are very undesirable for a hydrogen store and much work has been carried out to try and reduce the desorption temperature. [8]

Under inert conditions $LiBH_4$ desorbs hydrogen by the reaction described:

$LiBH_4 \rightarrow LiH + B + (3/2)H_2$ when heated to 600°C (1) [9]

Equation (1) determines only 13.8 wt% of H_2 may be desorbed from $LiBH_4$ when heated to 600°C. Zuttel et al found approximately 0.3 wt% was desorbed in the low temperature phase structure, and a further 13.5 wt% was able to be desorbed in the more prominent high temperature phase with peaks at 350°C and 500°C. This totals 13.8 wt% of hydrogen removed from $LiBH_4$ by conventional heating, a further 4.5 % mass of hydrogen remains within the LiH decomposition product. [10] Further heating to above 680°C, the melting point of LiH, would be required to desorb this further 4.5 wt% H_2. [9]

2.2.3 Conventional Heating Additions

Due to the high temperatures required, many groups have attempted to both increase the desorption kinetics of $LiBH_4$ and to catalyse the reaction. Zuttel et al documented that when SiO_2 powder was introduced to pure $LiBH_4$ the desorption temperature significantly decreased. [10]

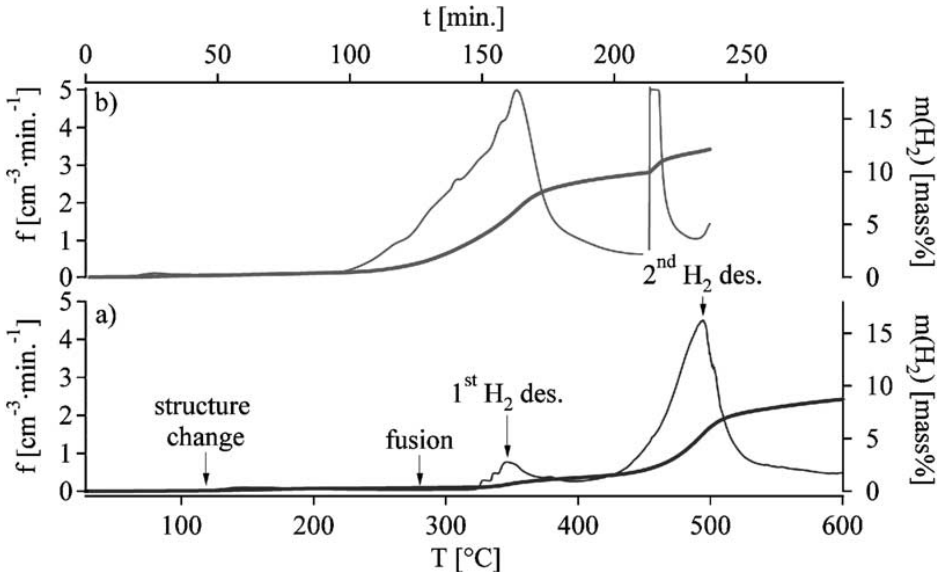

Figure 4 –

Desorption of Hydrogen in $LiBH_4$, a) uncatalysed reaction, b) catalysed reaction with SiO_2 powder [10]

Figure 4 (b) demonstrates the reduction in temperature for all 3 hydrogen desorption peaks. A small desorption occurs before 100°C, however the catalysed desorption beginning at 200°C now becomes the dominant desorption peak with 9 wt% of hydrogen being desorbed before 400°C. A sharper peak is observed at approximately 450°C which desorbs the rest of the hydrogen totalling 13.8 wt% of hydrogen removed.

Zuttel et al documented that the SiO_2 catalysed $LiBH_4$ desorption can be described as follows:

1. Structural transition at T = 108°C:

$LiBH_4 \rightarrow LiH_{4-\varepsilon} + B + \frac{1}{2}(\varepsilon)H_2$ (2)

2. First hydrogen peak starting at T = 200°C:

$LiBH_{4-\varepsilon} \rightarrow$ "$LiBH_2$" + $\frac{1}{2}(1-\varepsilon)\ H_2$ (3)

3. Second hydrogen peak starting at T = 453°C:

"$LiBH_2$" $\rightarrow LiH + B + (3/2)H_2$ (4) [10]

Although "$LiBH_2$" has not been identified as yet, the 9 wt% desorption below 400°C suggests such a compound is present. [10] The same wt% of hydrogen is removed from both catalysed and uncatalysed reactions and the temperatures are still too high for a practical vehicular hydrogen store. However the catalysed reaction does offer large energy savings compared to the un-catalysed reaction. With the introduction of other materials it may be possible to increase reaction kinetics and reduce the desorption temperatures further.

Au et al examined other possible $LiBH_4$ additions such as Mg, Al, $MgCl_2$ and $TiCl_3$ shown in figure 5. [11]

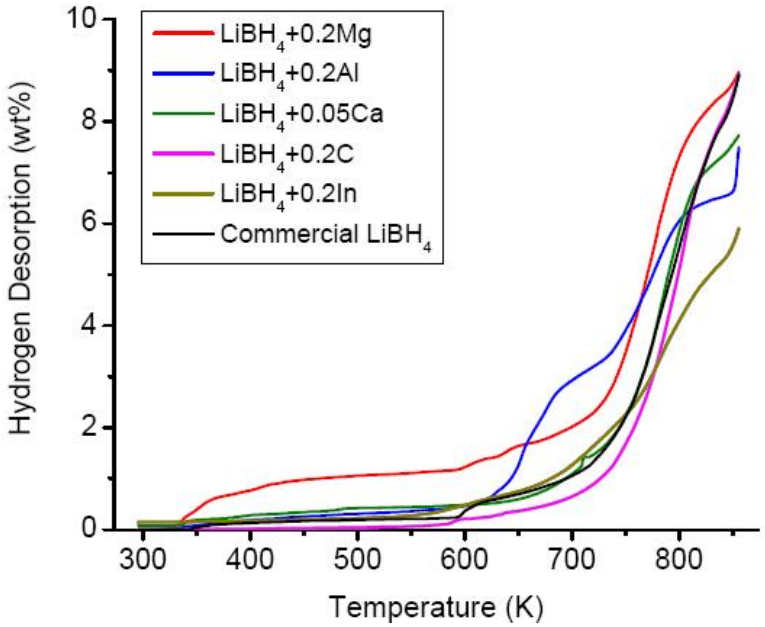

Figure 5 – TPD heating of $LiBH_4$ doped with various materials at 5°C / min under near-vacuum conditions of less than 5 mbar argon (a) [11]

Aluminium has a limited effect in reducing a major part of the hydrogen desorption temperature by approximately 50°C. Magnesium, however, allows a small hydrogen desorption to begin at 70°C and a major desorption to occur 30°C before as received $LiBH_4$ at around 420°C. $LiBH_4$, $MgCl_2$ and $TiCl_3$ mixed together in quantities of 1 : 0.1 : 0.1 respectively allows a significant and constant hydrogen desorption to occur between 100°C and 400°C, however only 5 wt% of hydrogen in the material is desorbed compared to 9 wt% for as received $LiBH_4$. Reducing the ratio of $MgCl_2$ and $TiCl_3$ to 0.076 and 0.047 respectively allowed 6.5 wt% of hydrogen to be desorbed, although the desorption began 100°C later, at approximately 200°C.

2.2.4 Recombination of $LiBH_4$

Although this thesis is not directly concerned with rehydrogenation of $LiBH_4$, it is important to briefly examine the recombination process to determine the potential of $LiBH_4$ as a hydrogen store.

Figure 6 – Recombination of as received and doped $LiBH_4$ after desorption, at 600°C and 100 bar H_2 for 45 minutes [12]

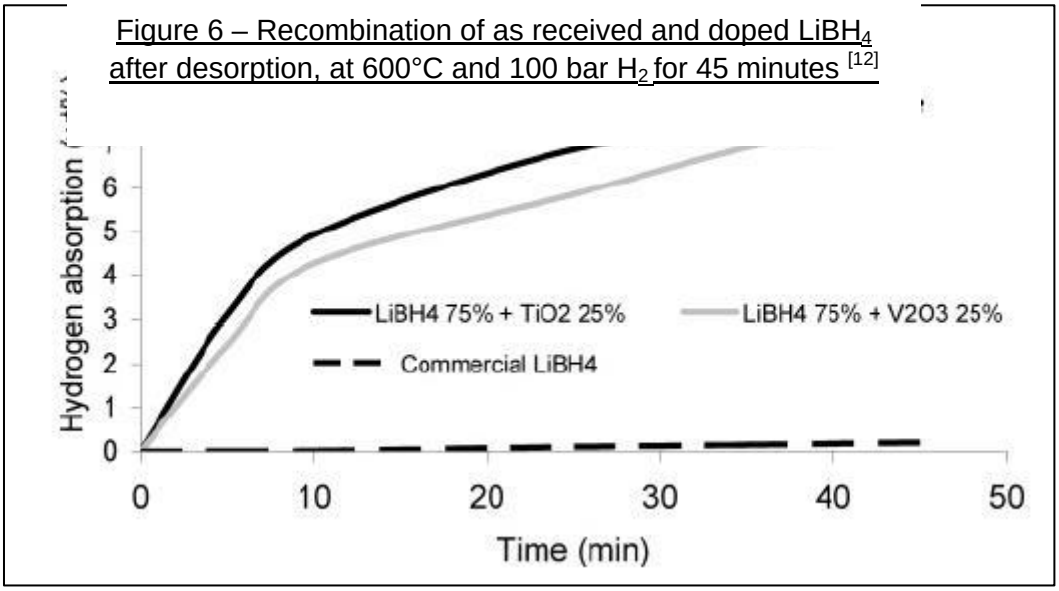

Au et al examined the rehydrogenation of as received and doped $LiBH_4$ after hydrogen desorption had occurred by heating the samples to 600°C. Figure 11 shows the relatively poor rehydrogenation of as received $LiBH_4$, where less than 0.2 wt% of hydrogen was recombined at 600°C and 100 bar H_2. [12] This poor level of reversibility is not suitable for a hydrogen store.

Au et al then examined the rehydrogenation of $LiBH_4$ doped with TiO_2 and V_2O_3, this yielded a large increase in hydrogen absorption within the materials, absorbing 7.8 and 7.9 wt% respectively. [12] Further refining of sample mixtures and other additions would be highly beneficial to increase reaction kinetics, H_2 absorption, and to decrease both temperatures and pressures of the operating system.

2.2.4 Conventional Heating of TiH_2

Hydrogen in TiH_2 accounts for 4.04 % of its total mass, however it is not a candidate storage material because it is too stable. Since TiH_2 will be added to $LiBH_4$ to create milled composites at different molar ratios, it is important to examine both the properties of TiH_2, and the properties of the $LiBH_4$: TiH_2 composites for standard Temperature Programmed Desorption (TPD) heating.

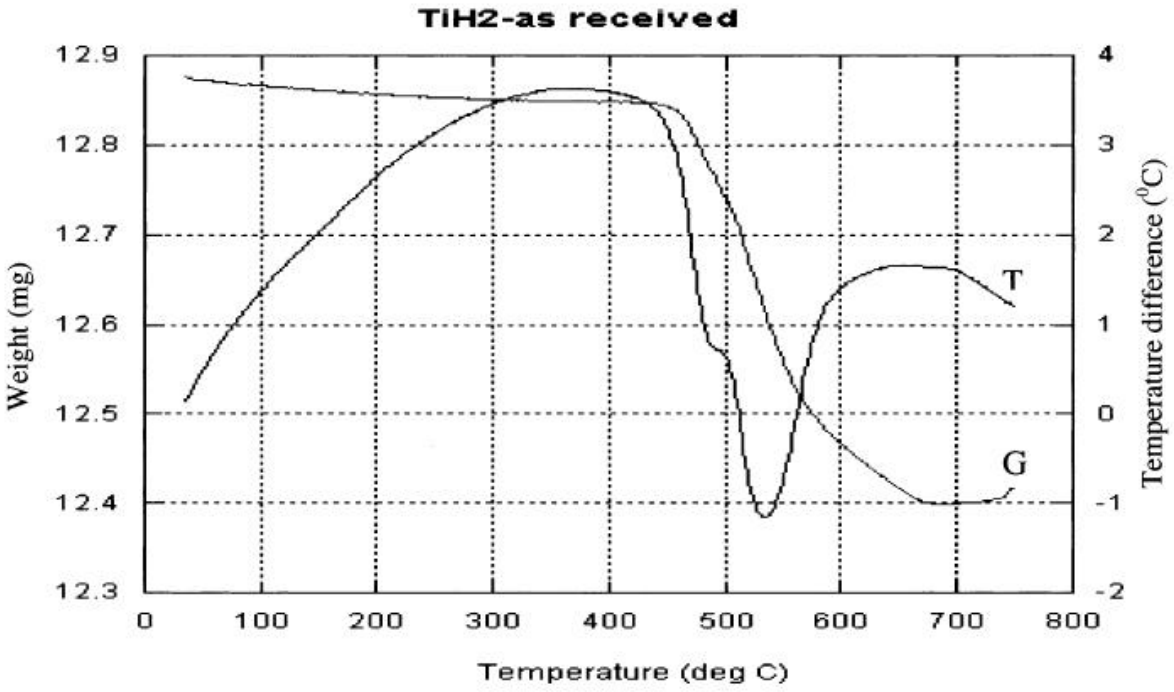

Figure 7 – TGA / DTA analysis of as received TiH_2 powder for TPD heating at 20°C / min [13]

Bhosle et al heated as received TiH_2 powder using TGA analysis at 20°C / min, as shown in figure 7. [13]

TiH_2 began to desorb hydrogen at approximately 480°C, continuing until 500°C, desorbing approximately 0.7 wt% of hydrogen in its first phase desorption. A second

phase desorption then occurred between 500 – 675°C, with approximately 2.7 wt% of hydrogen being desorbed from the sample. In total, 3.4 wt% of H_2 was desorbed from the TiH_2 powder. The DTA analysis identifies more clearly this two phase hydrogen desorption, the peak transformation temperature is unidentifiable in the first phase (due to the overlapping of the phases), and 535°C in the second phase.

TiH_2 was determined to follow a 2-phase desorption sequence as follows :

$TiH_2 \rightarrow TiH_x \rightarrow \alpha\text{-}Ti$ (5) [13]

The evaluation of "x" proved inconclusive in the as received TiH_2 powder, due to the overlap of the phases. Bhosle et al also examined the dehydrogenation of milled TiH_2 powders, shown by figure 8.

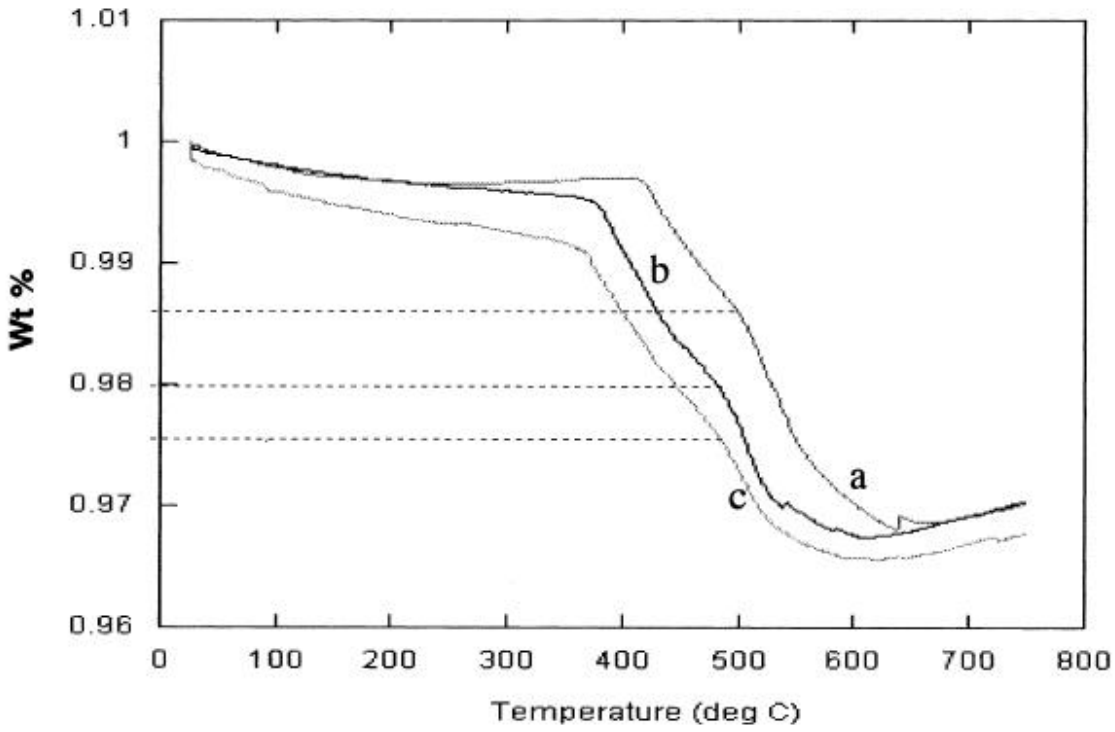

Figure 8 – TGA analysis of TiH_2 powders milled for a) 2 min b) 15 min c) 240 min [13]

V. Bhosle et al milled as received TiH_2 powders in a SPEX 8000 high energy ball mill for varying time intervals. TiH_2 was found to fragment at a fast rate during ball milling.

The as received TiH_2 had an initial particle size of 40 µm, however after a short period of milling the particle size saturated around 10 µm. [13]

As shown by figure 8, using TGA analysis, TiH_2 powders that were milled began hydrogen desorption at a lower temperature than the as received TiH_2, which began its first phase desorption at approximately 480°C. The powders milled for 2 minutes, 15 minutes and 240 minutes, began desorption at approximately 420°C, 390°C and 380°C respectively. The amount of hydrogen desorbed from the powders milled for 2 and 15 minutes was approximately 3.4 wt%, this was consistent with the desorbed wt% of hydrogen from the as received TiH_2. The TiH_2 powder milled for 240 minutes desorbed slightly more hydrogen at approximately 3.5 wt%. [13]

Referring to equation (5), although the two phase desorptions again overlap, Bhosle et al calculated the value of "x" for the second phase hydride desorption of TiH_x.

Milling Time	x values in second hydride phase
2 minutes	1.1
15 minutes	0.9
240 minutes	0.7

Table 2 – Value of x in TiH_x phase as a function of milling time [13]

Bhosle et al concluded that the TiH_x phase is formed by the partial degradation of TiH_2, with the value of x being dependent on the particle size, this phase is more thermally stable at high temperatures than TiH_2 due to the larger activation energy required for decomposition. The lower hydrogen content in the finer particles was determined to be an effect of the increased surface area of the hydride. TiH_x was found to be unstable at

low temperatures, and subsequently the phase transforms into a combination of (TiH_2 + α-Ti) phases, therefore TiH_x was not able to be identified using XRD analysis. [13]

2.2.5 $LiBH_4$ and TiH_2 mixed composites

Yang et al examined the desorption profiles of $LiBH_4$ mixed with various metals and metal hydrides, for the addition of TiH_2, the thermodynamically preferred products are given by equation (6).

$$2\ LiBH_4 + TiH_2 \rightarrow TiB_2 + 2\ LiH + 4\ H_2 \quad (6)$$ [14]

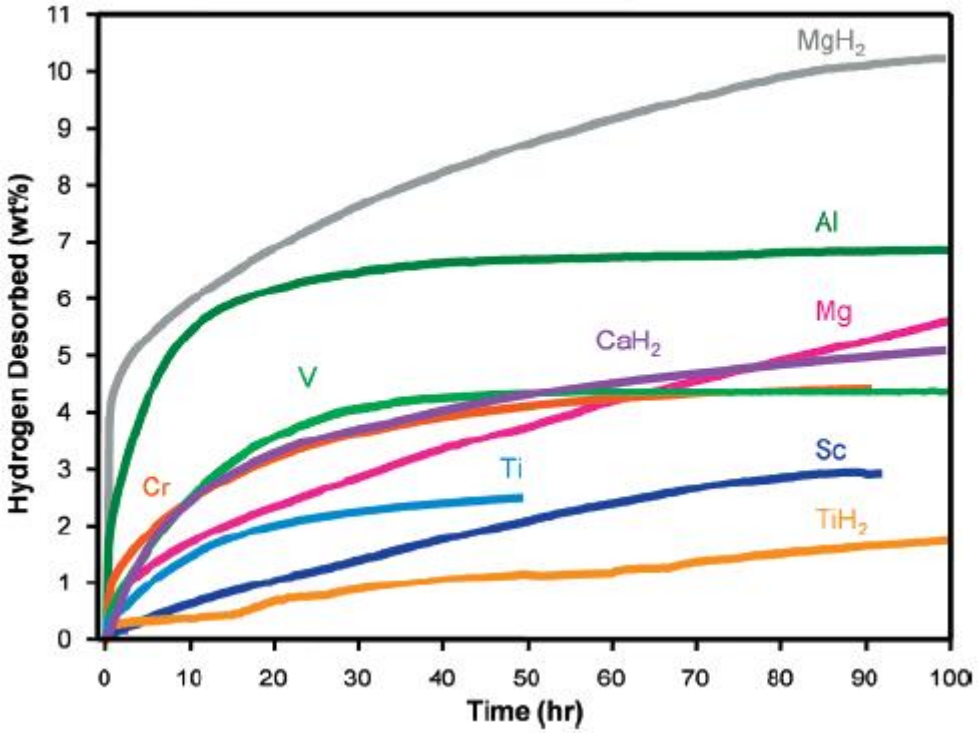

Figure 9 – Isothermal kinetic desorption data for $LiBH_4$ with various metal and metal hydride additions using PCT apparatus at 1 bar H_2 and 400°C [14]

Referring to figure 9, $LiBH_4$ was mixed with various metals and metal hydrides, and then heated to 400°C at 1 bar H_2 for isothermal kinetic desorption to occur, for up to 100 hours. Figure 14 shows that isothermal kinetic desorption of the TiH_2 : $LiBH_4$ composite is not consistent with the formation of a metal boride product. [14] Less H_2 was desorbed from the $LiBH_4$: TiH_2 composite than expected, with only 1.7 wt% of hydrogen desorbed after 100 hours, compared to a theoretical desorption of 8.6 wt% if the materials had formed the thermodynamically preferred products.

Yang et al concluded the TiH_2 additive did not thermally destabilise $LiBH_4$; there was however a modest improvement in kinetic properties, such as reduced desorption temperatures and improved desorption rates. Kinetic attributes of TiH_2 determine that the thermodynamically preferred products for desorption of the $LiBH_4$: TiH_2 composite is not accessible, and that $LiBH_4$ doped with TiH_2 will desorb according to equation (1), with B, H_2 and LiH being the desorption products. [14]

2.3 Microwave Irradiation

2.3.1 Microwave Theory

Although it may be possible to significantly reduce the desorption temperature of $LiBH_4$ further with the introduction of more effective catalysts, it would be a great benefit if large energy savings could be made from more efficient heating techniques. Work has recently begun into microwave radiation into absorbent materials, allowing for improved reaction kinetics and faster desorption profiles for many hydrogen storage materials. It would be beneficial if microwave radiation could be investigated to determine its suitability for use with hydrogen storage media.

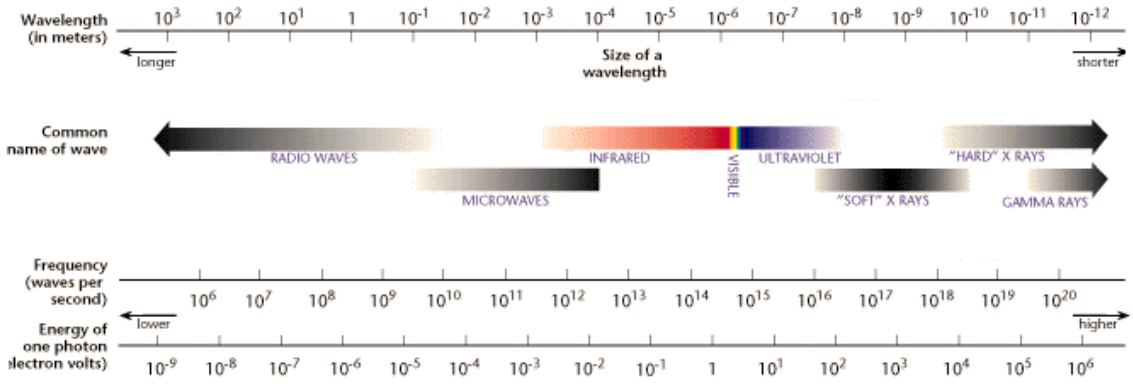

Figure 10 – The electromagnetic spectrum [15]

Microwaves are electromagnetic waves at frequencies between 0.3 and 30 GHz situated between radio-waves and infra-red in the electromagnetic spectrum. Most commercial microwave ovens operate at a frequency of 2.45 GHz and wavelength 12.24 cm, in the industrial sector, 0.915 GHz of wavelength 33.3 cm is predominantly used. [16]

Microwave processing of materials offers a different approach to conventional heating. Currently microwave appliances have been developed for communications, cooking food, tempering and thawing wood, and heating rubber materials. Microwave irradiation offers many advantages over conventional heating, allowing materials to be rapidly and uniformly heated; this uses far less energy than conventional heating methods which rely on diffusion of heat from the particle surfaces. [17]

It is important to understand how microwaves interact with a material. Many microwave effects are not completely understood, such as increased reaction rates and unique properties in specific materials, therefore examining and understanding this interaction could allow for these advantages to be utilised with greater effectiveness. [18]

2.3.2 Microwave Interaction

Microwave heating differs from conventional thermal processing since electromagnetic waves are directly absorbed within the molecules of a material causing them to increase in temperature, compared to the regular heating effects such as conduction, convection and radiation. This microwave effect is known as 'volumetric heating' since it is possible for the entire volume of bulk material to be heated. [19] Materials are able to be defined in 4 categories relating to their microwave characteristics:

- Transparent – microwaves pass through material with little or no attenuation (low dielectric loss)
- Opaque – microwaves cannot penetrate the material and are reflected (high dielectric loss)

- Absorbing - material absorbs microwave energy depending on dielectric loss factor
- Mixed absorber – multi phase material with both high-loss and low-loss phases, which allows for selective heating that cannot be achieved by conventional heating

Microwave heating in materials occurs due to two properties: the dielectric constant, which is the ability for the material to allow polarization, and the dielectric loss which pertains to the inability of the material to follow the reversals of the electromagnetic field. [20]

Power generated by microwave irradiation can be defined as follows:

$P = 2\pi f E^2 \varepsilon''$ (7)

Where P = power

f = frequency

E = electric field strength

ε'' = dielectric loss

Assuming the frequency and electric field strength remained constant, the higher the dielectric loss of the material, the more power is generated and faster heating will occur within the material.

2.3.3 Microwave Heating of Materials

Single Mode and Multi Mode Applications

There are two distinct types of microwave systems, single and multi mode. Microwaves are electromagnetic waves which move between positive and negative values shown by figure 11.

Figure 11 – Microwave wave function [21]

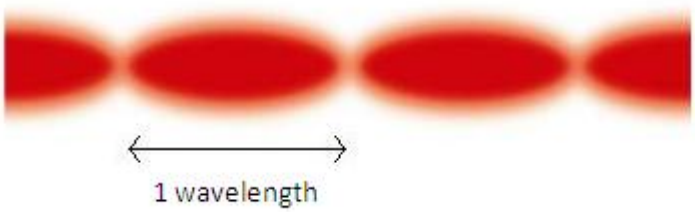

At some points along this wave the power generated will be zero; this is not favourable for a microwave system which tries to deliver maximum power to the material. Since microwaves have relatively large wavelengths (in the order of centimetres) it is possible to design a microwave cavity which measures exactly one wavelength, meaning at the centre of the cavity, maximum power will be generated by the single wave. This is known as a single mode system and can be used to process small samples (in the order of milligrams). The energy distribution is homogenous throughout the cavity.

However for some applications this type of system is not suitable, for example processing large bulk materials would result in only the centre being significantly heated. Multi-mode systems (such as a commercial microwave oven) employ many waves which are reflected around the microwave cavity by mode stirrers. This enables a large volume of material to be heated simultaneously with no restrictions upon the size of the cavity. However since this stirring process is somewhat random and difficult to measure, it is possible for many ‘hot spots’ or ‘cold spots’ to exist within the microwave cavity, where the total wave function for overlapping waves at a point is either at its maximum or minimum. For simple applications such as cooking food this has little effect, however for more complicated applications such as measuring precise

heating rates of small samples, even shifting the sample a few millimetres could result in significantly altered conditions making precise characterisation increasingly difficult. [21]

2.3.4 Microwave Applications

Microwave appliances are used to sinter ceramic materials and more recently metallic powders have been processed. Microwave processing offers significant advantages for sintering, since high temperatures (above 800°C) are usually required to complete the process, particularly for steel compositions which require temperatures of 1100-1300°C. Conventionally, to achieve and maintain these temperatures would use large amounts of energy since conventional thermal processing is very inefficient. [22]

2.3.4 Microwave Catalysis / The "Microwave Effect"

Mixed mode materials of differing dielectric properties can be useful for increasing reaction rates under microwave irradiation. Highly absorbing materials can heat surrounding microwave transparent particles as an indirect heat source. This becomes particularly useful if the absorbent material is catalytically active to help drive the reaction to completion. This technique is known as "microwave catalysis" and has been used successfully in many areas of research, particularly for ferromagnetic and paramagnetic materials. [16]

Many advantages of microwave processing are attributed to a "microwave effect" arising in thermal and non-thermal forms. Thermal microwave effects include kinetically favoured reaction products being formed at large heating rates which are

very difficult to reproduce for conventional heating techniques; this often produces larger yields than expected and increases processing quality. 'Hot spots' also cause certain areas of a material to be heated by a larger amount than areas nearby, on a molecular scale. This can result in catalytically active components being heated by a larger amount than by conventional heating which drives the reaction to completion more rapidly. Non-thermal effects include selective catalyst heating. Roussy et al found when a $BaBiO_{3-x}$ catalyst was irradiated, the increase in selective heating produced a decrease in oxygen production causing the catalyst to behave differently to conventional thermal processing. [23]

2.3.5 Microwave Heating of TiH_2, $LiBH_4$ and $LiBH_4$:TiH_2 composites

Due to microwave irradiation greatly increasing the speed of thermal processing, it would be desirable if microwave irradiation could be successfully applied to composites for hydrogen storage. Nakamori et al examined heating of various powder materials such as metal hydrides, (LiH, NaH, MgH_2, CaH_2, and TiH_2) and alkali borohydrides, ($LiBH_4$, $NaBH_4$, and KBH_4) by microwave irradiation at a frequency of 2.45Ghz in a multimode system. [24]

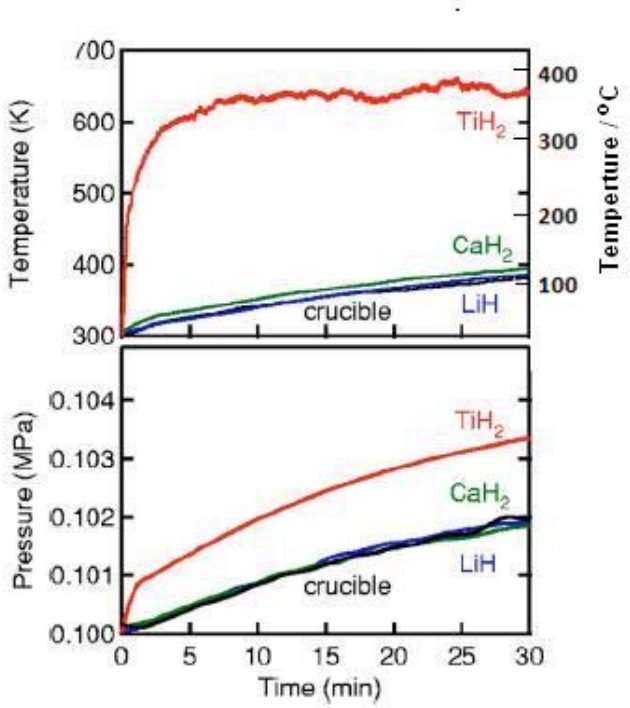

Figure 12 – Desorption of hydrogen from light metal hydrides due to microwave irradiation in an argon atmosphere [24]

Referring to figure 12, poor microwave heating was exhibited in LiH and CaH_2 reaching temperatures of approximately 125°C after 30 minutes of irradiation. It was determined that no hydrogen desorption occurred for these materials, since the pressure increase is consistent with when only the crucible sample holder was present during irradiation.

TiH_2 underwent rapid heating to over 325°C after less than 5 minutes of irradiation. Orimo et al determined the TiH_2 lattice had shrunk, with the crystal structure transformed from cubic to tetragonal. Some of the TiH_2 was transformed into a $TiH_{1.92}$ phase which was confirmed by XRD analysis, however only a small amount of hydrogen was desorbed. [24] Assuming that all of the TiH_2 would be converted to $TiH_{1.92}$ through microwave irradiation, this would only liberate a theoretical 0.16 wt% of hydrogen, however an even smaller wt% was desorbed by the TiH_2 sample. Orimo et al concluded that the particle size was larger than the penetration depth of the microwaves, therefore desorption only occurred from the surface area of the particles. [24] TiH_2 was found to exhibit rapid heating under microwave irradiation due to conductive loss which will be examined later when the dielectric properties of the material are considered. In a microwave application TiH_2 would not be useful for a hydrogen store, however it would make an ideal susceptor material for other hydrides which have a larger wt% of hydrogen stored within the hydride.

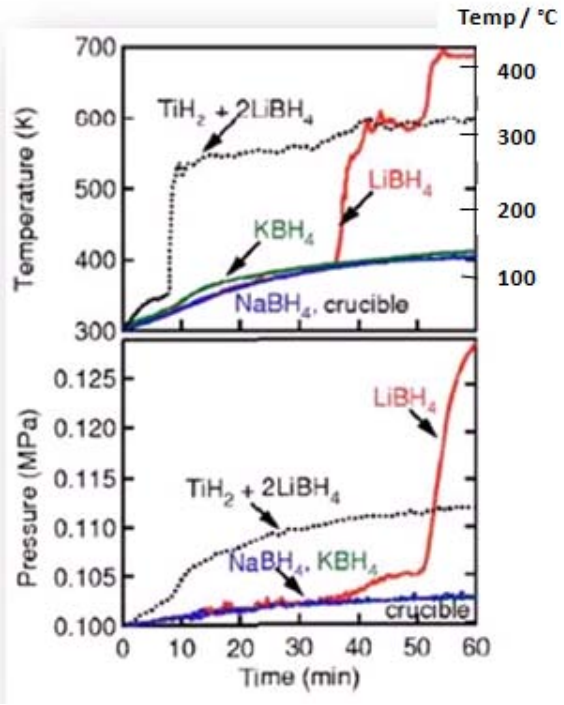

Figure 13 – Desorption of hydrogen from alkali borohydrides due to exposure to microwave irradiation in an argon atmosphere [24]

Figure 13 shows the desorption of alkali borohydride samples when exposed to microwave irradiation for up to 60 minutes. KBH_4 and $NaBH_4$ exhibited poor heating rates, however $LiBH_4$ rapidly heated between approximately 35 and 40 minutes of irradiation to over 300°C, at this point it can be inferred that hydrogen is being desorbed with a small pressure increase of 0.003 MPa. A further heating ramp occurred after 50 minutes of irradiation with $LiBH_4$ being heated to approximately 420°C, the temperature then remained constant for the remaining 10 minutes of irradiation, corresponding to a larger pressure increase of 0.025 MPa.

When $LiBH_4$ and TiH_2 were milled together and irradiated in a 2:1 molar ratio respectively, a very steep heating ramp occurred after 8 minutes from approximately 75°C to 250°C within 1 minute, together with an increase in pressure. The composite then continued to heat slowly to approximately 320°C corresponding to a total pressure increase of 0.0125 MPa after 60 minutes of irradiation. This increase in pressure is again inferred to be due to hydrogen desorption. To understand this large heating ramp of the milled $LiBH_4$:TiH_2 composite it is important to examine the dielectric properties of both TiH_2 and $LiBH_4$.

2.3.6 Dielectric properties of $LiBH_4$ and TiH_2

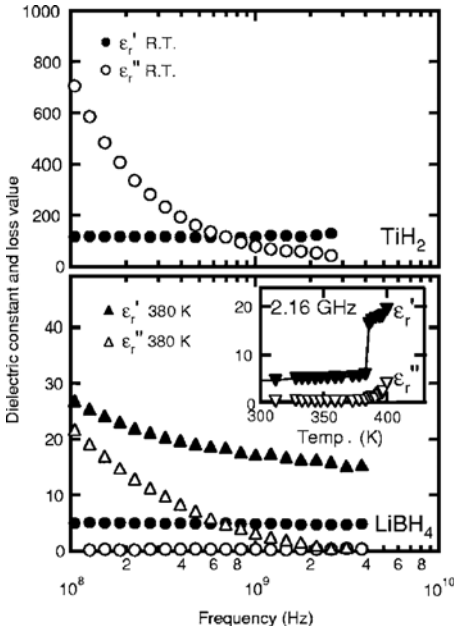

Figure 14 a / b – Dielectric constants of TiH_2 / $LiBH_4$ at room temperature and 380K

Where

ε' = Dielectric constant

ε''= Dielectric loss factor [24]

Figure 14a shows the dielectric properties of TiH_2, figure 14b the dielectric properties of $LiBH_4$. At room temperature across a frequency range of 0.1GHz to 4GHz, the dielectric loss is far larger for TiH_2 ranging from approximately 700 to 50, compared with approximately zero for $LiBH_4$ across the frequency range. This shows that TiH_2 is a metallic conductor which heats up through microwave irradiation due to conductive loss. Referring back to equation (7); the larger the dielectric loss, the larger the power produced resulting in increased heating rates.

In contrast, at room temperature $LiBH_4$ acts as an insulator with a dielectric constant of 5 and loss factor of approximately zero over the frequency range. However at 107°C, the dielectric constant and dielectric loss values of $LiBH_4$ increase from 5 to 20 and 0.1 to 5 respectively, between 100°C and 125°C, at a frequency of 2.16 Ghz. This increase is consistent with the increased heating ramp shown in figure 13 at this temperature. This change in dielectric properties occurs at the same temperature as the structural transition of $LiBH_4$: the orthorhombic structure of $LiBH_4$ changes to a

hexagonal configuration, and so it can be inferred that the shift in dielectric properties of $LiBH_4$ is due to this structure change.

$LiBH_4$ and TiH_2 both heat under microwave irradiation due to conductive loss, while materials such as MgH_2 and $NaBH_4$ have the dielectric properties of insulators throughout heating and therefore show no significant increase in temperature. [25]

Since TiH_2 has favourable dielectric properties for microwave irradiation and $LiBH_4$ desorbs large volumes of hydrogen upon microwave heating, Orimo et al mixed the two powders to create a composite in a 2:1 molar ratio of $LiBH_4$ and TiH_2 which exhibited the partial behaviours of both materials; 5.2 wt% of the material was removed through hydrogen evolution after 30 minutes of irradiation. [24] TiH_2 acts as a microwave susceptor to heat the surrounding $LiBH_4$; this benefits the desorption of $LiBH_4$ since it reaches its desorption temperature far faster than would be possible with conventional heating techniques.

Further work by Orimo mixed $LiBH_4$ with elemental B and C to create various composites which were then irradiated shown by figure 15.

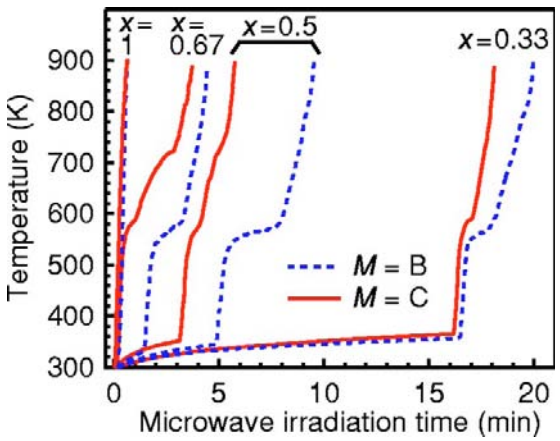

Figure 15 – Changes in temperature due to microwave irradiation for (1-x)$LiBH^4$ + xM (Where M= B or C) [26]

Using composite mixtures of $LiBH_4$: C and $LiBH_4$: B of 1 : 0.6 respectively, 6 wt% of material was removed due to hydrogen desorption in under 5 minutes, this offers significantly quicker heating periods than the $LiBH_4$: TiH_2 composites. [26]

This large increase in heating rates offers the potential for large energy savings and allows for greater control of hydrogen evolution once the properties of the composite have been examined. Shorts bursts of electromagnetic radiation could be employed for a far more efficient and faster hydrogen evolution to match power demands more easily. It is possible to create different properties for a composite by either altering the ratio of the powders to be mixed, or to alter the mixing techniques which are described in the next section.

2.4 Milling Techniques

Various techniques exist to mix powders together including simple powder mixing and mechanical milling. These techniques allow composite materials to exhibit different characteristics due to varying homogeneity of mixed particles and differing grain and particle sizes.

Simple powder mixing is a low energy technique allowing for materials to be sufficiently mixed together without altering grain or particle size of the composite, this can be particularly useful if multi-phase materials need to be examined without altering their initial physical properties.

Milling powders together offers a far more energy intensive mixing technique which significantly alters grain and particle size of the milled composite. Stainless steel balls are placed inside a milling pot which is then rotated, there are various type of mills and many factors which determine the properties of the milled composite:

- type of mill
- milling container
- milling speed
- milling time
- type, size, and size distribution of the grinding medium
- ball-to-powder weight ratio
- milling atmosphere
- temperature of milling

[27]

Planetary mill is a particularly highly energy intensive type of ball milling where 4 milling pots rotate around a central axis, the milling pot and supporting plate rotate in different

directions causing the milling balls to run along the surface of the wall for a duration of time, causing a grinding effect on the powder medium. The milling balls also leave the surface and collide at high speeds with the other side of milling pot, this significantly alters grain and particle size of the material and can be considered a high energy collision.

Roller milling is a far less energy intensive milling technique than planetary milling. The stainless steel balls are typically much smaller, the milling pot rotates around its central axis and the resulting collisions occur at lower velocities. This is still considered to be high energy in comparison to simple mixing, but offers a significantly lower energy intensive milling technique than planetary milling.

2.5 Conclusions of Literature Review

The introduction of a hydrogen economy may help the UK lower its carbon emissions. However without a viable hydrogen storage material it would not be possible to introduce hydrogen-powered vehicles which could compete commercially with gasoline fuelled internal combustion engines. For this to occur, a material must have: a high wt% of hydrogen, fast reaction kinetics and a low desorption temperature to allow the easy liberation of hydrogen fuel. It must also be of a reasonable cost.

$LiBH_4$ is able to store 18.5 wt% of hydrogen, however it is a stable material requiring large desorption temperatures above 450°C for significant hydrogen desorption; it also exhibits poor reaction kinetics and reversibility. Current techniques of doping $LiBH_4$ with catalysts such as SiO_2 and MgH_2 have been partially successful allowing for a significant reduction in desorption temperatures, however further research must be conducted to reduce temperature further. Au et al conclude that the thermodynamic stability of $LiBH_4$ is able to be destabilised by the introduction of various metal hydrides and metal chlorides; however the rehydriding temperatures and hydrogen pressures required for recombination remain high, with slow reaction kinetics. [11] This indicates that thermodynamic reversibility of $LiBH_4$ is low and rehydriding may be a much more difficult process than the initial desorption.

TiH_2 is able to store 4.04 wt% of hydrogen, this material is even more stable than $LiBH_4$, requiring temperatures in excess of 680°C to achieve significant hydrogen desorption using conventional heating techniques; it is therefore not considered to be a suitable hydrogen store. It does however, have favourable dielectric properties for microwave irradiation.

Microwave irradiation offers an alternative heating technique to conventional thermal processing, allowing the material to be volumetrically heated offering the potential for a far smaller energy input and producing faster heating rates. $LiBH_4$ has poor dielectric properties to allow for large heating rates through microwave irradiation, so susceptor materials with high dielectric losses must be introduced to allow for selective heating within the material; this is not achievable by conventional heating. It will be important to examine different composite mixtures of $LiBH_4$ and susceptor materials, particularly TiH_2, C and B which have high dielectric losses and act as thermal conductors. Many microwave properties including thermal effects and microwave catalysis should be examined to drive the fastest heating rates to produce increased yields and quality in production of the end product with significant energy savings. Non thermal effects such as selective catalyst heating should also be studied.

3. Aims and Objectives

The aim of the project was to examine the differences between conventional heating and microwave heating techniques used to desorb hydrogen from $LiBH_4$ and $LiBH_4$ composite-mixtures.

$LiBH_4$ and TiH_2 were to be milled in different molar ratios using planetary and ball milling techniques. These starting materials and milled composites were then to be characterised by scanning electron microscopy and x-ray diffraction to determine their initial properties.

Differential scanning calorimetry and thermo-gravimetric analysis techniques were then to be used to determine the desorption profiles (under Argon) for all starting materials and milled composites.

A Hydrogen Disproportionation Desorption Recombination (HDDR) rig and microwave system would then make a direct comparison between conventional (TPD) and microwave heating techniques under the same atmospheric conditions; they both employ the same gas sorption system and similar loading mechanisms. This would enable an assessment to be made into the usefulness of microwave technology in solid-state hydrogen storage. The acronym HDDR will be used henceforth in this thesis.

4.1 Experimental Method

4.1.1 Starting Materials

The starting materials used were:

$LiBH_4$ 95% purity, d 0.666 purchased from Sigma-Aldrich.

TiH_2, 98% purity, -325 mesh, F.W 49.93, d 3.910 purchased from Sigma-Aldrich.

4.1.2 Material Processing

Samples were weighed out in an argon glovebox, then mixed together in different molar ratios of 1:1, 2:1 and 3:1 $LiBH_4$: TiH_2, to create a total sample weights of approximately 6 – 10 g. Each mixture was placed in a 430 cm^3 stainless steel roller milling pot using stainless steel balls measuring 6 mm in diameter and a powder-ball ratio of 33:1. This was sealed in an argon atmosphere, it was then milled for 20 minutes on a Pascall 1601 Roller Mill for two 10 minute durations at 200 rpm, with a 10 minute rest time in-between the milling periods. The rest time was to ensure the sample did not unnecessarily heat due to the friction during the milling process, which would have possibly resulted in hydrogen desorption.

The 2:1 $LiBH_4$: TiH_2 mixture was also placed in a 500 cm^3 stainless steel planetary milling pot using stainless steel balls measuring 14 mm in diameter and a powder-ball ratio of 66:1. This milling pot was again sealed under 1 bar argon and placed on a Retszch PM400 Planetary Ball Mill. The mixture was milled for 30 minutes at 300rpm for three 10 minute durations, with a 10 minute rest time in-between each spell, again to prevent unnecessary heating of the sample.

4.2 Characterisation

4.2.1 Scanning Electron Microscopy

A JEOL 6060 SEM was used to examine particle size of the starting materials, and milled $LiBH_4$ and TiH_2 composites. Secondary mode was used to record the images of the samples. Samples of approximately 5 mg were inertly mounted onto carbon discs measuring 1 cm in diameter.

4.2.2 X-Ray Diffraction

A Phillips X'pert XRD was used to examine the composition of the starting materials, milled composites, and the milled composites after hydrogen desorption. The scanning 2θ range was between 20 - 120° using Cu K_α radiation at a scanning rate of 1º / min. The samples were prepared in an argon glove box, by placing the powders onto small plastic slides and covering them with sellotape. This isolated the samples from the air once they were removed from the glovebox.

4.3 Conventional Heating Desorption Profiles

4.3.1 Differential Scanning Calorimetry (DSC) and Thermo-Gravimetric Analysis (TGA) pan testing

Before any TGA or DSC analysis was performed, the volatility of $LiBH_4$ and TiH_2 was assessed; this was to determine if any damage would be caused to the instruments by the material bubbling over the sides of the alumina TGA pot or aluminium DSC pot. Pan testing was completed in a simple furnace tube which was inertly loaded in an argon glove box. This was then placed inside a furnace tube and connected to a rotary and diffusion pump. The pot was heated under vacuum to the required temperature at 15°C / min, the maximum heating rate the furnace could achieve.

4.3.2 Thermo-Gravimetric Analysis

Thermo-gravimetric analysis was carried out on a Netzsch 209 IRIS TGA. An alumina TGA pot was inertly loaded in an argon glovebox with approximately 2 - 4 mg of sample and placed in the TGA machine; it was heated to both 450°C and 500°C at 2°C / min. The pressure of the chamber was 1 bar argon (g) using a flow rate of 40 ml / min. The amount of hydrogen desorbed was inferred from a mass measurement of the sample as a function of temperature.

Each TGA pot was calibrated to remove buoyancy effects, where gas inside the pot would expand upon heating causing spurious mass measurement readings. The calibration was conducted by heating the empty TGA sample pot up at a specific heating rate to the required temperature, in this case at 2°C / min to both 450°C and 500°C.

c-DTA analysis was also performed using the TGA equipment. This is a mathematical calculation routine based on the temperature measurement of the sample. Endothermic and exothermic effects can slightly influence the temperature during heating and cooling. By making a comparison of the actual temperature change of the sample against the theoretical temperature change, these effects can be detected and quantified.

4.3.3 Differential Scanning Calorimetry

Differential scanning calorimetry was performed on a Netzsch 409 HP DSC. The difference in the amount of heating for the aluminium sample pan and empty aluminium reference pan showed any energy changes, such as phase transitions or gas desorption in exothermic or endothermic reactions. The sample was inertly loaded in an argon glovebox with approximately 3 - 3.5 mg of sample, and heated to 550°C at 2°C / min. The pressure of the chamber was 3 bar argon (g) using a flow rate of 100 ml / min.

The DSC was calibrated by using an empty DSC pan and heating it to 550°C at 2°C / min, the conditions in which the sample would be measured.

4.4 Conventional Heating in Differential Gas Sorption System

4.4.1 HDDR Experimental Setup

Two systems were built which used the same gas flow system in an attempt to minimise differences in operating conditions, the first of these was the HDDR rig pictured in figure 16.

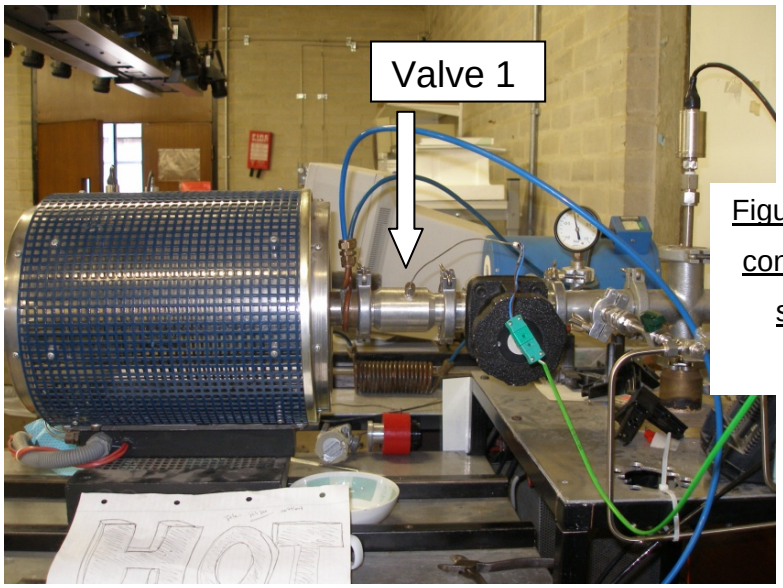

Figure 16 – HDDR Rig connected to the gas sorption system

This rig consisted of a furnace tube connected to the gas flow system and a rotary pump. The furnace tube was able to be inertly loaded by closing valve 1 shown in figure 16 and by removing the clamps holding the tube, this was then loaded into the argon glovebox. A test tube with a sample placed inside was then loaded into the furnace tube, as shown in figure 17.

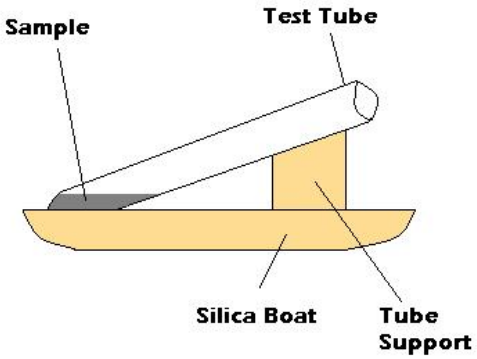

Figure 17 – HDDR rig sample loading tube

The sample was loaded into the test tube which was placed upon a silica boat, this was supported at an angle by a silica mould to stop the sample from bubbling out during the experiment.

Valve 1 was re-attached and removed from the glove box maintaining the argon atmosphere, the furnace tube was re-attached to the gas sorption system and the connecting pipes were evacuated using the rotary pump before exposing the furnace tube to the HDDR system. This was to ensure that the sample was never exposed to air at any point in the experiment and also, that hydrogen was never mixed with air which could create an explosive mixture. The furnace had a maximum heating rate of 10°C / min. A K-type thermocouple was placed inside the furnace tube as close to where the sample would be positioned as possible.

The gas sorption system is controlled by two mass flow controllers which can modify their input / output to keep the system at a desired pressure and flow rate, these controllers are operated by a computer system. A schematic for the gas sorption system is shown in figure 18.

System Operating Mode 1:

Differential Gas Sorption

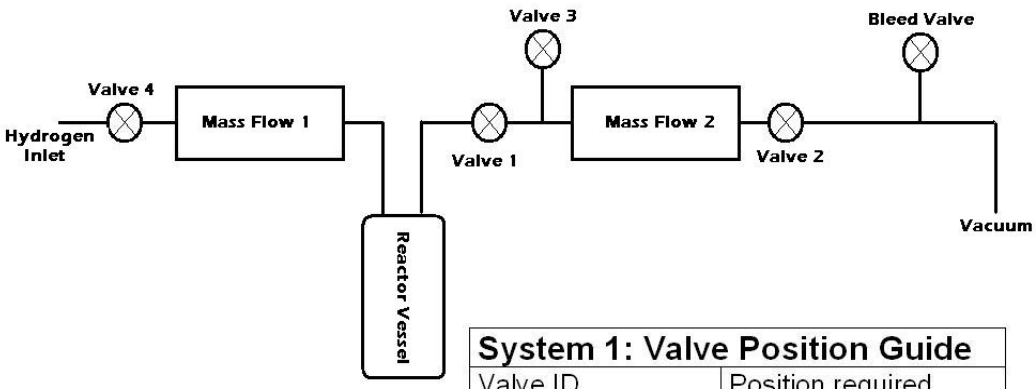

System 1: Valve Position Guide	
Valve ID	Position required
1	A
2	A
3	0
4	1

Figure 18 – Schematic Diagram of Gas Sorption System

Once all valves are opened, the system's pressure is controlled by the input of mass flow controller 1 and the output of mass controller 2. The bleed valve can be set to a pre-determined pressure and will vent all gas above this pressure in case of malfunction of the mass flow controllers.

4.5 Microwave Heating in Differential Gas Sorption System

The microwave system can be connected to the same gas sorption system as the HDDR rig by removing the HDDR fittings and connecting them to the microwave sample tube. The building of this microwave system was led by Rob Bell as part of an EngD project, (School of Metallurgy and Materials, University of Birmingham). Figure 19 once again shows the placement of the microwave reactor vessel within the gas system.

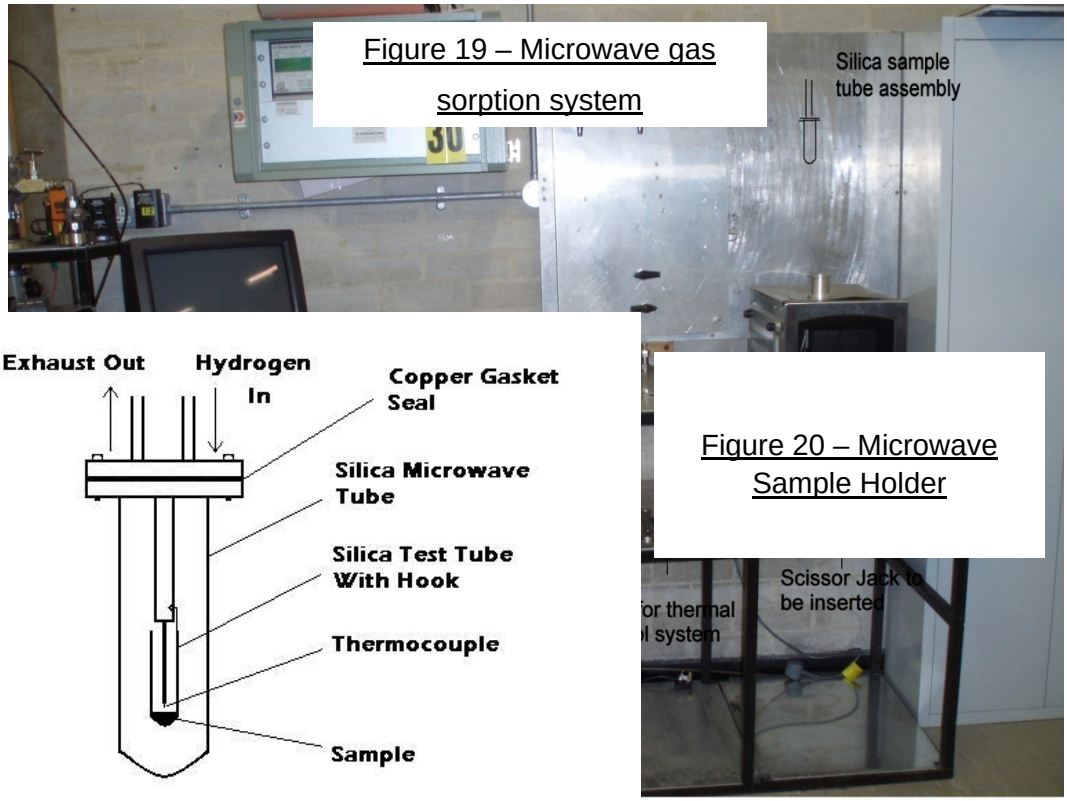

Figure 19 – Microwave gas sorption system

Figure 20 – Microwave Sample Holder

A hole was drilled in the side of a commercial Panasonic 900W inverter microwave through which a silica tube could be inserted, silica was used since it is almost completely transparent to microwaves. The tube was welded to a stainless steel clamp with a cutting edge which compresses a copper gasket to create an air tight seal, this allows the tube to be inertly loaded in an argon glovebox.

A second silica test tube was placed within the microwave tube to hold the sample, this was suspended from the thermocouple casing. The K type thermocouple was placed as close to the sample as possible to provide as accurate a reading of temperature during irradiation as possible. Since microwave heating can cause large heating ramps, it was necessary to suspend the inner silica test tube so that it made no contact with the outer silica glass to prevent damage. Rapid increases in temperature were expected to fracture the inner silica tube which is readily replaceable, however to replace the thicker outer tube requires welding a new tube back onto the stainless steel clamp, this would be a lengthy, costly process.

Since previous efforts to design hooks using various metals had caused damage to the microwave tubes due to rapid heating, a glass blower crafted the hooks by melting the tops of the silica test tubes and moulding the silica into shape.

A conical flask filled with 100ml of de-ionised water of known dielectric loss was placed at the bottom of the microwave cavity, this allowed for microwave absorption to occur even if the sample itself was not absorbing. This prevented the internal wiring from overheating.

The microwave appliance had 3 distinct power modes, high, medium and low. According to the manufacturer's specifications, this related to power ratings of 900, 450 and 225 Watts respectively.

5. Results and Discussion

5.1 Sample Preparation

$LiBH_4$ and TiH_2 were mixed in various molar ratios using both roller and planetary milling techniques to produce various composites.

Three samples were roller milled for 20 minutes in total, at 200 rpm. This was conducted in two 10 minute milling periods with a 10 minute rest time in-between cycles; this was to prevent unnecessary heating of the powder due to friction during the milling process which may have caused hydrogen to desorb. The powders were mixed in molar ratios of 1 :1, 2:1 and 3:1 of $LiBH_4$: TiH_2, using a 33:1 ball to powder ratio for a sample weight of approximately 4 - 10 g.

The 2:1 $LiBH_4$: TiH_2 was also planetary milled for 30 minutes in total, at 300 rpm using a 66:1 ball to powder ratio, the sample weight was approximately 10 g. This was conducted in three ten minute milling periods with 10 minutes rest between cycles, again to prevent unnecessary sample heating. Since these two milling techniques offer greatly different energy intensities during milling, it was determined that the milling time and ball to powder ratio need not be consistent for both techniques. These composites are listed below in Table 3.

Sample	Composition	Milling Type	Total Milling Time/mins
RL1	2:1	Roller	20
RL2	1:1	Roller	20
RL3	3:1	Roller	20
PL1	2:1	Planetary	30

Table 3 – Composition of the milled composites

5.2 SEM Analysis of Starting Materials and Milled Composites

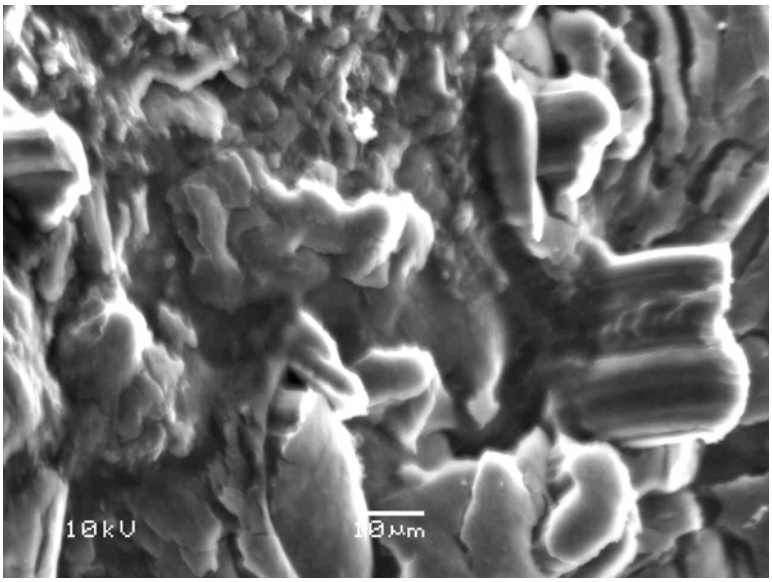

Figure 21 – SEM Secondary mode image of $LiBH_4$

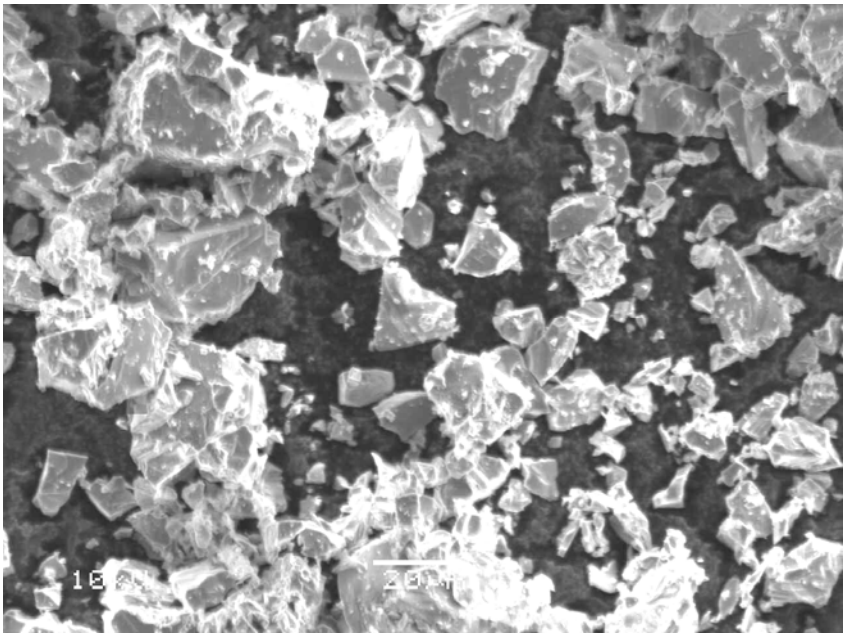

Figure 22 – SEM Secondary mode image of TiH_2

Comparisons of figure 21 and 22 demonstrate the large size of the $LiBH_4$ particles compared to the TiH_2 particles. $LiBH_4$ exhibits particle sizes of up to 50 µm or greater compared with TiH_2 particles of approximately 20 µm.

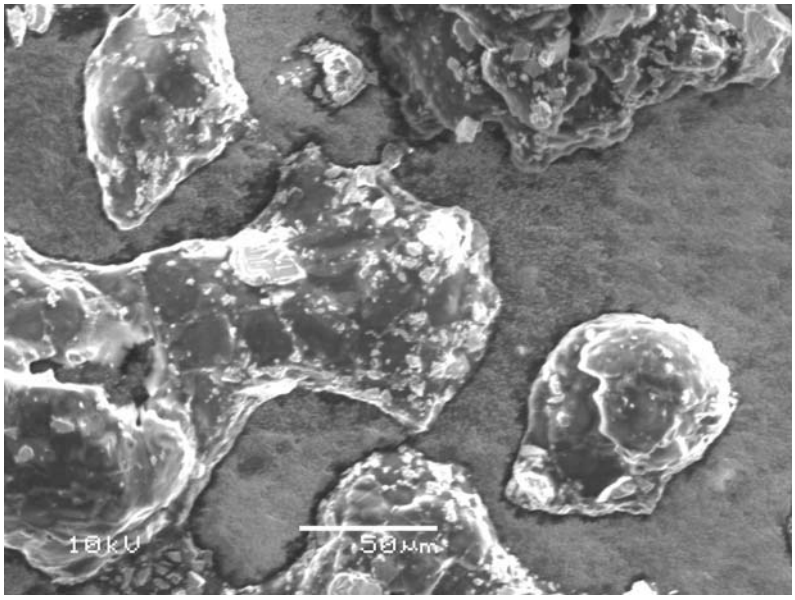

Figure 23 – SEM Secondary mode image of RL1 2:1 $LiBH_4$:TiH_2 Milled Composite

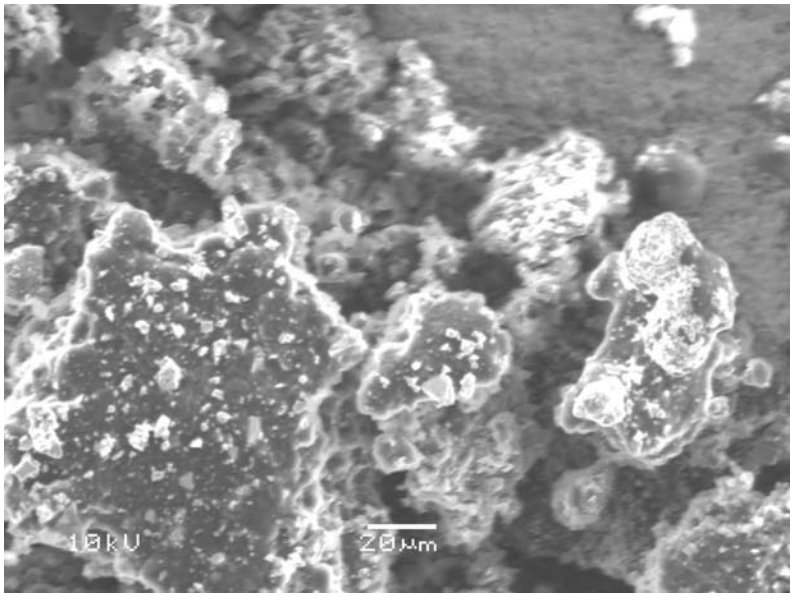

Figure 24 – SEM Secondary mode image of PL1 2:1 $LiBH_4$:TiH_2 Milled Composite

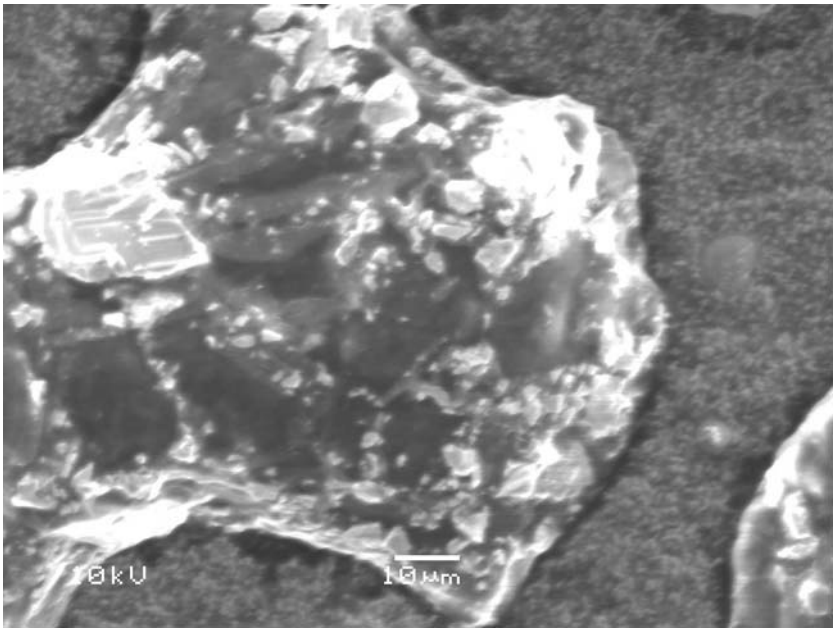

Figure 25 – SEM Secondary mode image of RL1 2:1 $LiBH_4$:TiH_2 Milled Composite

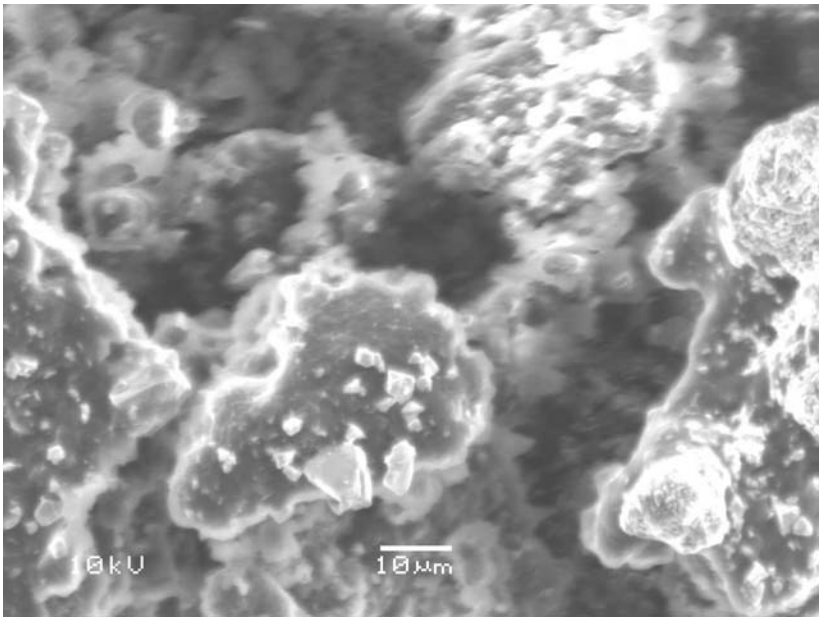

Figure 26 – SEM Secondary mode image of PL1 2:1 $LiBH_4$:TiH_2 Milled Composite

A roller milled sample of 2:1 $LiBH_4$:TiH_2 powder is shown in figures 23 and 25. The supposition can be made, that the smaller TiH_2 particles are randomly distributed around the larger $LiBH_4$ clusters; the TiH_2 particle size seems to be significantly reduced to 5 µm or less. It would have been useful to confirm this by using Energy Dispersive Spectroscopy (EDS) which could have identified the different compounds.

Figures 24 and 26 show the planetary milled 2:1 $LiBH_4$:TiH_2 sample, the same random distribution of TiH_2 particles can be inferred to be present around the $LiBH_4$ clusters, however the grain size of the planetary milled particles is much smaller. The distribution is also more consistent than the roller milled sample, again the TiH_2 particles seem significantly reduced in size to less than approximately 3 µm.

The SEM secondary images suggest that both roller milling and planetary milling techniques allowed for significant mixing of both starting materials, so that TiH_2 would be able to act as an efficient susceptor material. However, the increased TiH_2 distribution in the planetary milled sample suggests that this technique would allow the TiH_2 in the composite to act as a more efficient susceptor material than in the roller milled sample.

Bhosle et al found larger reductions of TiH_2 particle size due to high energy ball milling. an initial 40 µm to 36 nm for 15 minutes of high energy ball milling. [13] It would have been useful to conduct EDX analysis to confirm the identity of each material, and to examine powders which had been milled for varying periods of time. This would have enabled a greater understanding into the differences between milling techniques, and to understand the change of particle size with respect to the milling period.

5.3 DSC/TGA Pan Testing

Since lithium borohydride is known to be a volatile, reactive material, it was necessary to heat samples in both DSC and TGA pans in a safe environment to assess the risk posed to both DSC and TGA machines. TiH_2 was also tested, however this substance was not expected to bubble or leak out of the DSC pan or TGA pot. All samples were run under near vacuum conditions using a rotary pump (approximately 10^{-3} mbar (a)) to prevent evolved hydrogen pressuring the system at high temperatures. The conditions, results and observations of the pan testing are listed below in Table 4.

Sample	Sample Size / mg	Type of Milling	Pans Tested	Max Temp / °C	Result	Observations
$LiBH_4$	10.05	none	DSC	400	Fail	DSC pan sealed shut, some $LiBH_4$ had bubbled out
$LiBH_4$	3.00	none	DSC	400	Fail	DSC pan sealed shut, some $LiBH_4$ had bubbled out
TiH_2	3.03	none	DSC	600	Pass	No bubbling or spluttering, pan lid easy to open
2:1 $LiBH_4$:TiH_2	2.97 / 3.07/ 2.96	roller	DSC & TGA Pan/ Crimped DSC pan	450	Pass	No bubbling or spluttering, pan lids easy to open
2:1 $LiBH_4$:TiH_2	2.97	roller	Crimped DSC pan	550	Pass	Very small amount of bubbling on top of pan, pan turned slightly black
3:1 $LiBH_4$:TiH_2	2.85 / 3.13 / 3.03	roller	DSC & TGA Pan / Crimped DSC pans	450	Fail/ Pass	DSC and TGA pans sealed shut, sample bubbled out to outside of pots. / Tiny amount of bubbling out of hole in top of crimped DSC pan but considered safe

Table 4 – TGA / DSC pan testing to examine the volatility of $LiBH_4$ and $LiBH_4$ composites

As received $LiBH_4$ was the first powder to be examined, a DSC pan with 10.05mg of pure $LiBH_4$ was heated under vacuum at the furnace's maximum heating rate of 15°C / min to 400°C where it was held for 30 minutes. When the pan was removed the $LiBH_4$ had bubbled out of the pan and sealed the lid shut, if this had been run in the DSC machine, the sample would have damaged the DSC thermocouple. The sample size was reduced to 3 mg since this would be the minimum weight of material which could produce an accurate DSC trace, the same result occurred and $LiBH_4$ was deemed unsafe to run to this temperature in the DSC machine.

3.03 mg of TiH_2 exhibited no bubbling or spluttering when heated to 600°C at 15°C/min and was determined to be safe for experimental runs.

2:1 and 3:1 ratios of $LiBH_4$: TiH_2 were then examined. Approximately 3 mg of 2:1 RL1 sample did not bubble or splutter during both heating runs to 450°C using a DSC pan and TGA pot. However, approximately 3 mg of the 3:1 RL3 sample, which had a larger lithium content, failed the heating runs for both pans; the sample bubbled out of the sides of the pan and sealed it shut. It was considered unsafe to run the 3:1 sample in the TGA without finding alternative TGA pot materials such as tantalum.

DSC pans were able to be crimped round the outside with pliers once the sample had been loaded and a small hole was made in the lid of the pan to allow gas to escape. This crimping method allowed for any escaping liquid sample to be vented from the top of the pan where it would cause least damage to the equipment. 3 mg samples of 2:1 and 3:1 ratios of roller milled $LiBH_4$: TiH_2 were heated in crimped DSC pans to 450°C and 550 °C at 15°C/min, both pans exhibited little or no bubbling of liquid from the top of the pan, it was therefore deemed safe to run samples in the DSC using this crimping technique.

5.4 XRD Analysis on Starting Materials

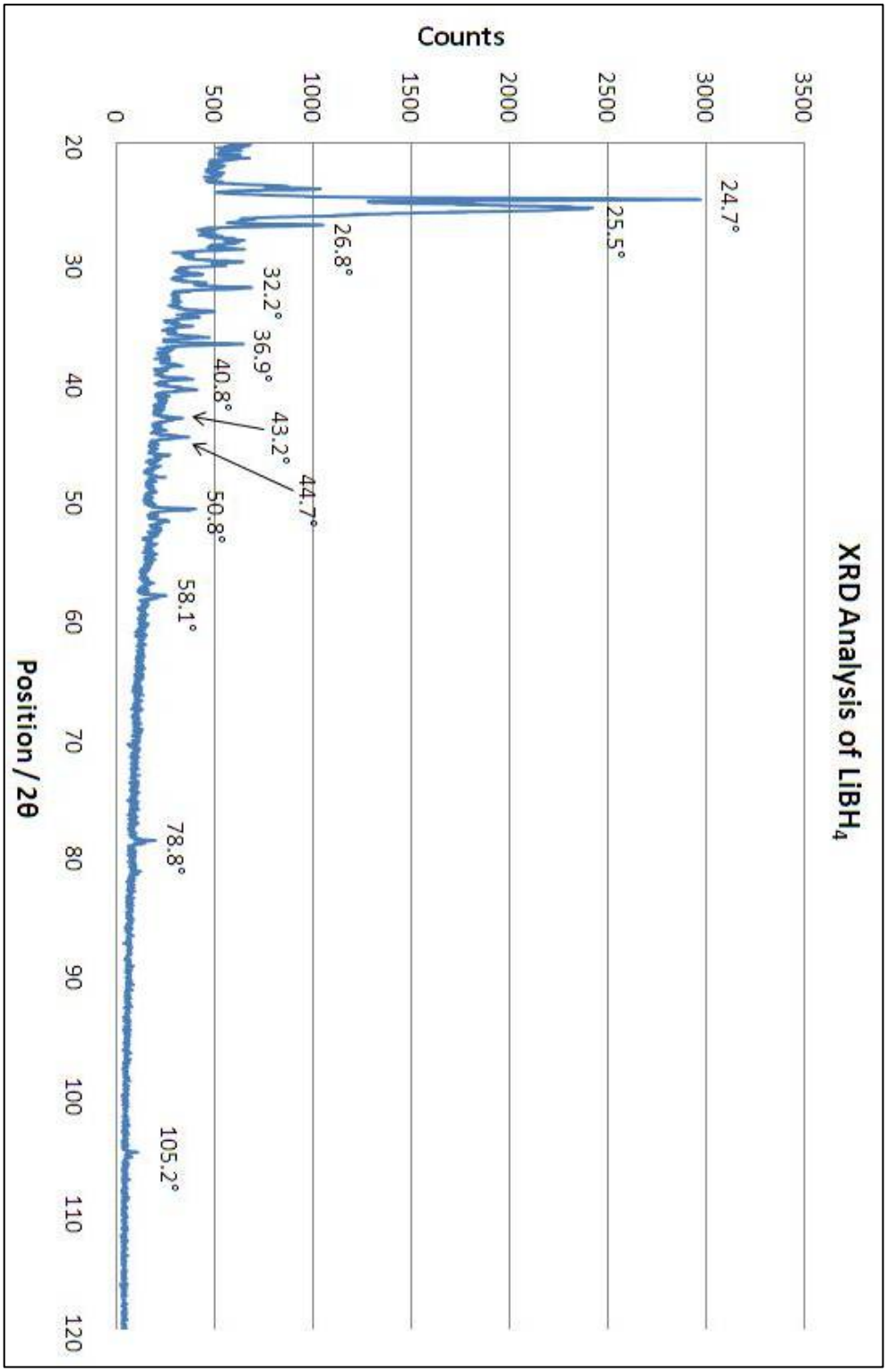

Figure 27 – XRD Analysis of as received $LiBH_4$ before heating

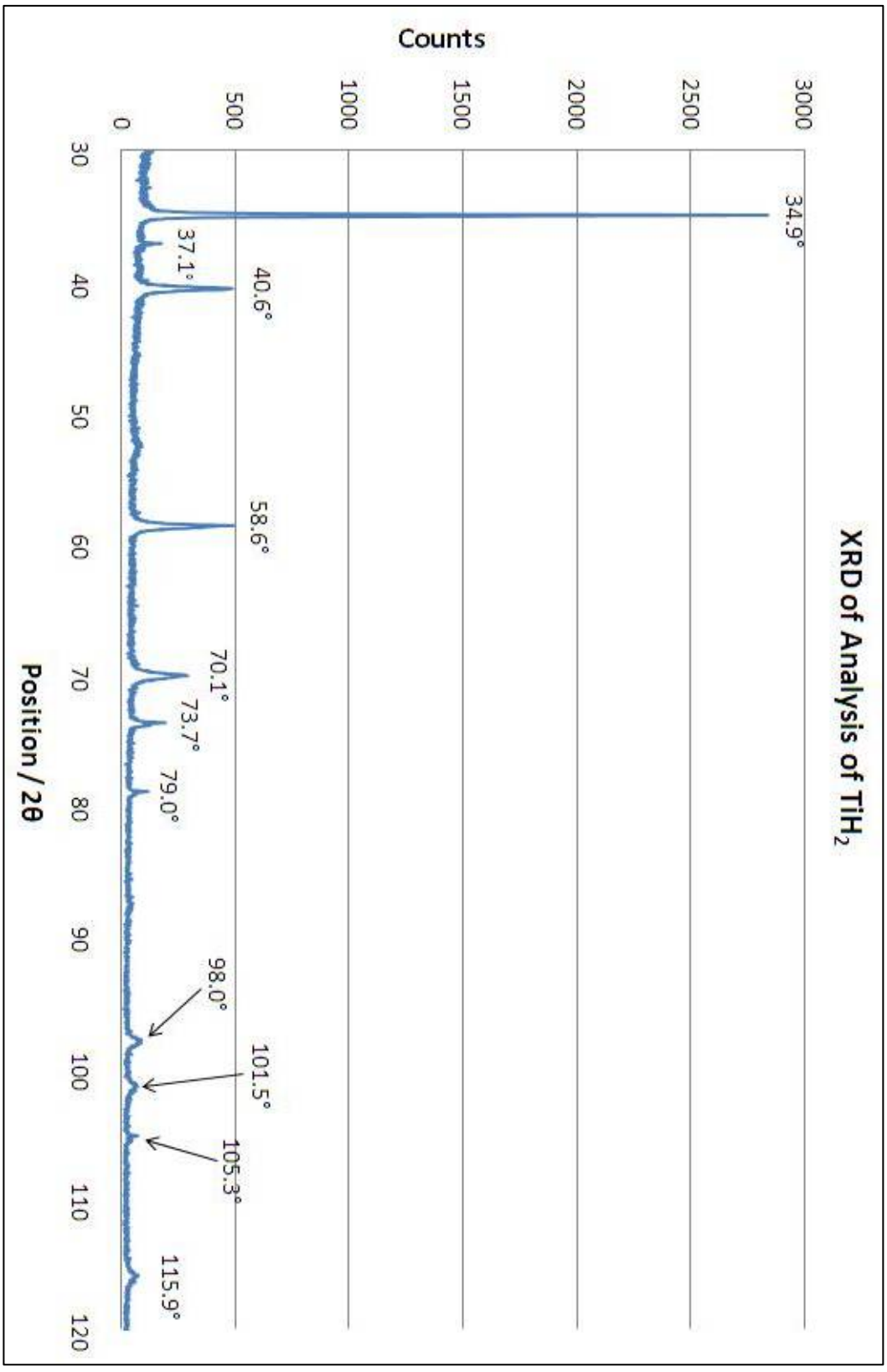

Figure 28 – XRD Analysis of as received TiH_2 before heating

Lithium borohydride is clearly identifiable by the XRD spectra in figure 27, in its orthorhombic phase structure. Since XRD was conducted at room temperature, no peaks were present for $LiBH_4$ in its high temperature hexagonal phase, this was consistent with XRD spectra documented by Zuttel et al for polycrystalline $LiBH_4$. [7]

After indexing it was confirmed that the peak at ~ 25.5º of 2θ was due to the sellotape which housed the sample. This peak was present in all XRD spectra and was not considered in the analysis.

TiH_2 was identified by XRD analysis in figure 28, in its tetragonal phase structure. Peaks for its cubic structure were not present, which exists experimentally above 30°C. These peaks were consistent with Orimo et al's XRD analysis of TiH_2. [24]

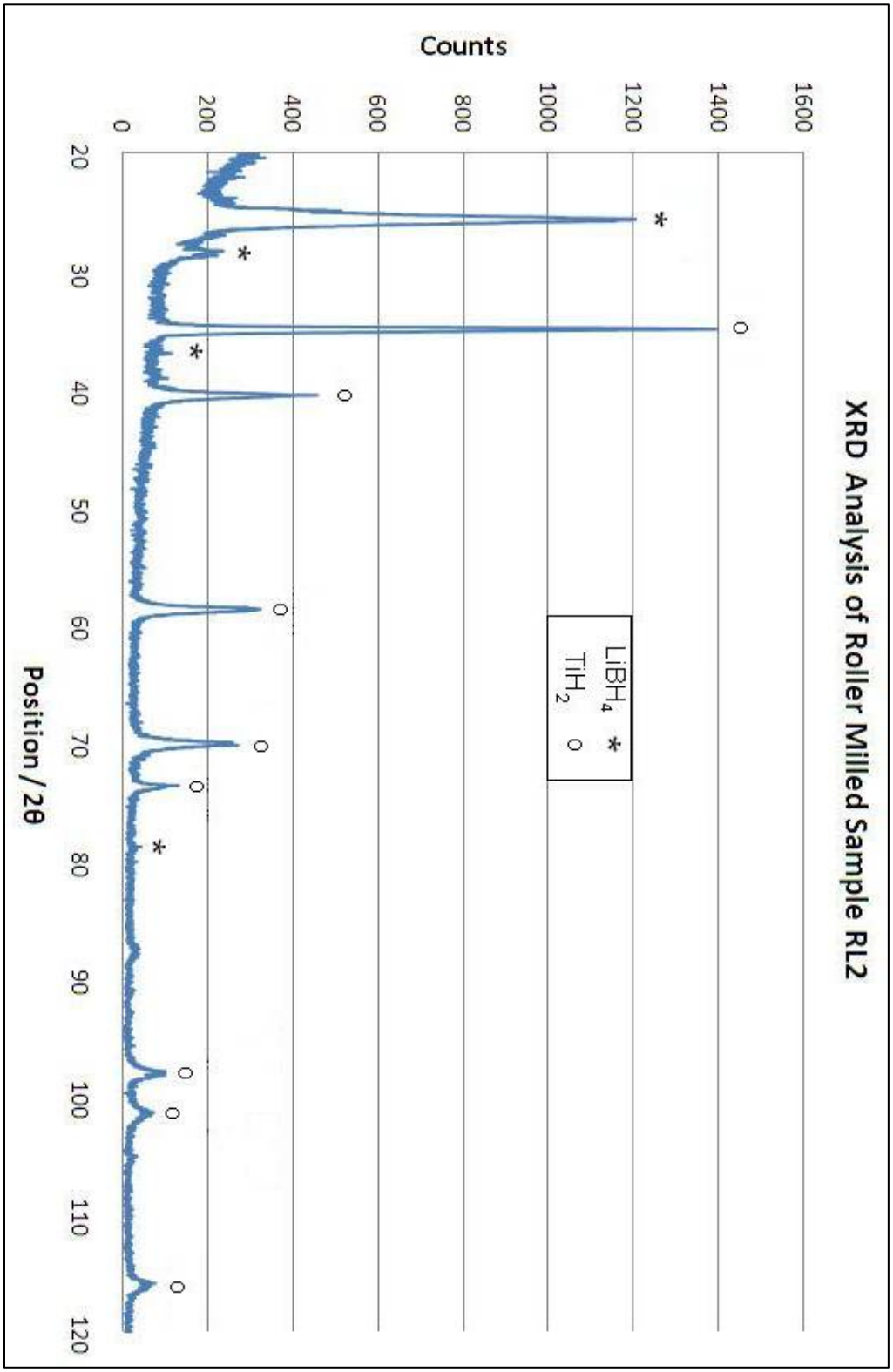

Figure 29 – XRD Analysis of milled composite RL2 (1:1 $LiBH_4$:TiH_2) before heating

Shown by figure 29, the 1:1 $LiBH_4$: TiH_2 rolled milled sample RL2 shows evidence of peaks for both $LiBH_4$ in its orthorhombic phase structure and TiH_2 in its tetragonal phase structure. No new peaks were observed, suggesting that no reaction had occurred between the two substances during mechanical milling. However, many $LiBH_4$ peaks for the milled $LiBH_4$: TiH_2 composite were either unidentifiable, or significantly lower in intensity than the XRD spectra for as received $LiBH_4$. This would suggest a partial loss of $LiBH_4$ crystallinity which can occur due to milling.

Samples RL1, PL1, and RL3 all produced similar patterns exhibiting the presence of both TiH_2 and $LiBH_4$, however the accuracy of these measurements was not great enough to make comparisons between relative intensities of peaks due to the small sample size.

However, referring to figure 29, the peak width was greater for $LiBH_4$ than for TiH_2. This is a contradiction to the interpretation of the SEM data in which TiH_2 was considered to produce smaller particles after milling. It could be supposed that the grain size for $LiBH_4$ was smaller than that of TiH_2 even though the particle size was larger. However this could not be confirmed without SEM-EDS data which could have identified the different compounds.

It would have been useful to examine $LiBH_4$: TiH_2 composites which had been mixed together by simple mixing and by different milling periods, therefore this loss of crystallinity in $LiBH_4$ could have been more thoroughly examined.

5.5 TGA Analysis

TGA analysis was begun for sample RL1 of ratio 2:1 $LiBH_4$:TiH_2; a sample mass of 3.32 mg was used. The sample was inertly loaded in an argon glovebox and heated at 2°C / min to 450°C, since this had been confirmed to be safe by pan testing (section 5.3).

After heating it was observed that the pot had turned black and the lid was sealed shut. There was a small amount of powder which had also bubbled over the side of the pot. This was inconsistent with the previous pan testing which found heating to this temperature to 450°C at a higher heating rate of 15°C/min had been safe with pressures near vacuum. Therefore either the material acted differently under the 1 bar argon atmosphere, or the longer heating time (compared to a faster heating rate) had increased the volatility of the material.

Since the effects of the first run had not been particularly damaging, a second TGA experiment with a slightly smaller sample size of 3.13 mg was run. This produced another accurate TGA desorption trace, however after observing the pot after the experiment there had been significant boil over, the lid was sealed shut and the pot had once again turned black.

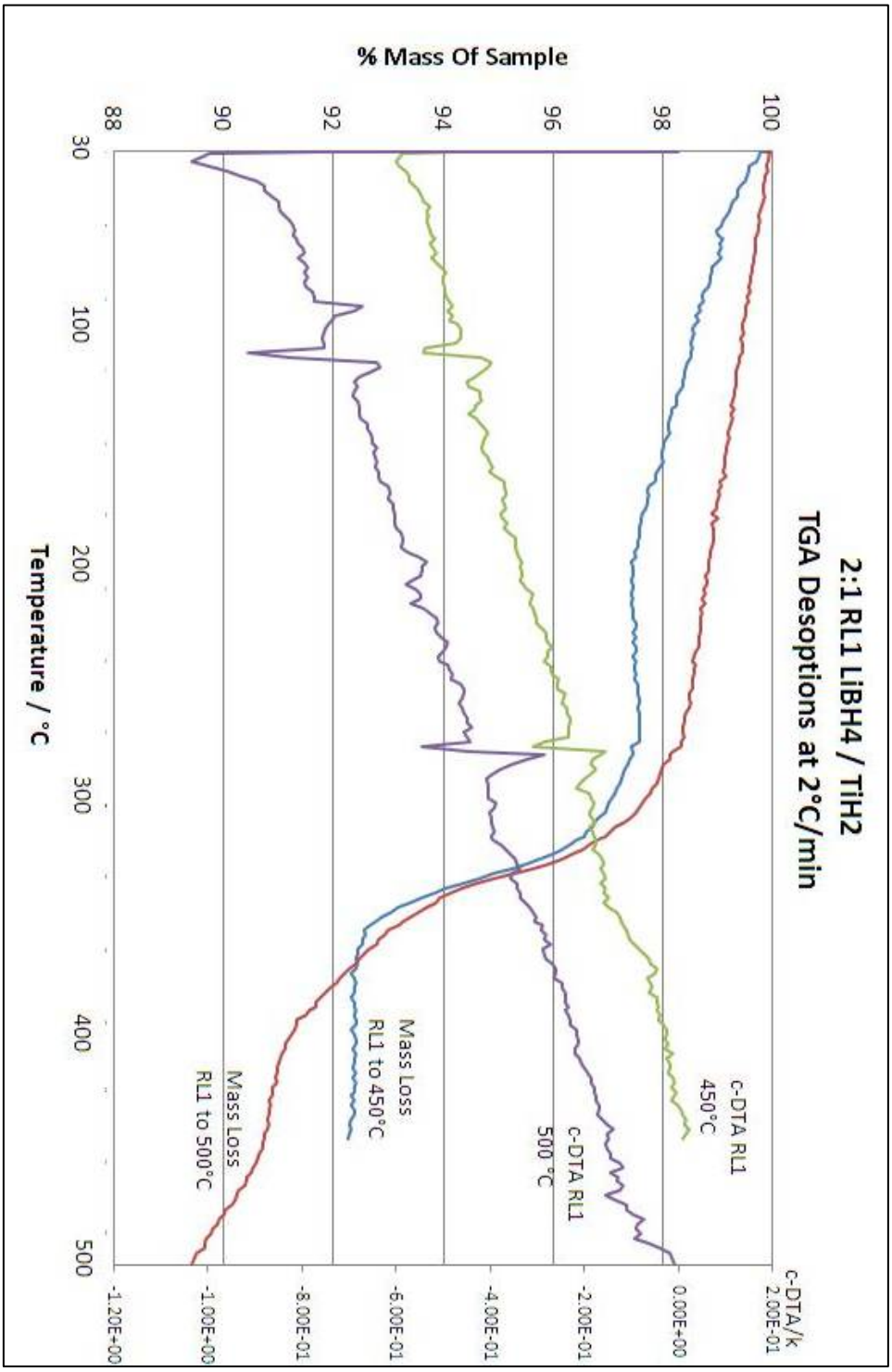

Figure 30 – TGA desorption profiles for 2:1 $LiBH_4$:TiH_2 roller milled sample RL1 heated to 450°C and 500°C at 2°C / min

The two desorption profiles for the RL1 sample heated to 450°C and 500°C are shown in figure 25. Accounting for errors in buoyancy calibration, it can be seen that the onset for desorption occurs around 280°C which is consistent with the point at which a fusion reaction occurs within $LiBH_4$. Zuttel et al documented a small desorption of 0.3 weight-% of as received $LiBH_4$, occurred at this temperature. [10]

However, the desorption exhibited in the RL1 sample begins 40°C earlier than observed by Zuttel et al (for the similar heating and flow rate conditions), at 280°C; approximately 4 weight-% of the RL1 sample is lost between 280°C and 380°C. Zuttel et al observed a 2nd hydrogen desorption of as received $LiBH_4$ which began at approximately 320°C, desorbing almost 5 weight % [10].

The reduction in desorption temperature for the $LiBH_4$: TiH_2 composite is consistent with work by Yang et al, who determined that the addition of TiH_2 to as received $LiBH_4$ caused improved reaction kinetics producing a modest reduction in desorption temperatures. [14]

Zuttel et al also observed a 3rd hydrogen desorption for as received $LiBH_4$, with an onset temperature at 450°C, this is consistent with the 2nd TGA run for the RL1 sample, which shows the beginning of this desorption. However, the temperature required to document the entire 3rd desorption of as received $LiBH_4$ would need be between 550 - 600°C.

Bhosle et al determined that as received TiH_2 exhibited a small hydrogen desorption at approximately 450°C with a phase change of $TiH_2 \rightarrow TiH_x$, where x is dependent upon the particle size, desorbing 0.7 wt% of hydrogen from TiH_2. [13] It was therefore unclear whether the desorption beginning at 450°C in figure 30 was due to $LiBH_4$ or TiH_2 desorption, or a combination of both.

Since the sample was already considered unsafe at 500°C, the sample size was once again lowered. This third TGA run was conducted with half the sample size of the previous experiment, using 1.64 mg of sample. The powder was once again heated at 2°C/min to 500°C, however this sample size proved not large enough to produce an accurate TGA desorption profile. After heating the pot was observed to still turn black and had foamed over the top with the lid sealed shut, even though the sample size was very small. It was concluded that the 2:1 $LiBH_4$: TiH_2 RL1 sample was not safe to be run in the TGA and another method to characterise hydrogen desorption by conventional heating should be considered.

c-DTA analysis of figure 30 shows two distinct features. The endothermic effect observed at 110°C is consistent with work by Zuttel et al [10] who determined this was due to polymorphic transformation of the $LiBH_4$. The second peak at approximately 280°C corresponds to a fusion reaction of the $LiBH_4$ which is accompanied by a significant desorption of hydrogen.

5.6 DSC Analysis

DSC analysis was carried out using crimped pans described earlier in section 4.3. 2.1 mg of sample RL1 was loaded into a crimped DSC pot (as described in section 5.3) and heated at 2°C / min to 550°C under 3 bar argon pressure.

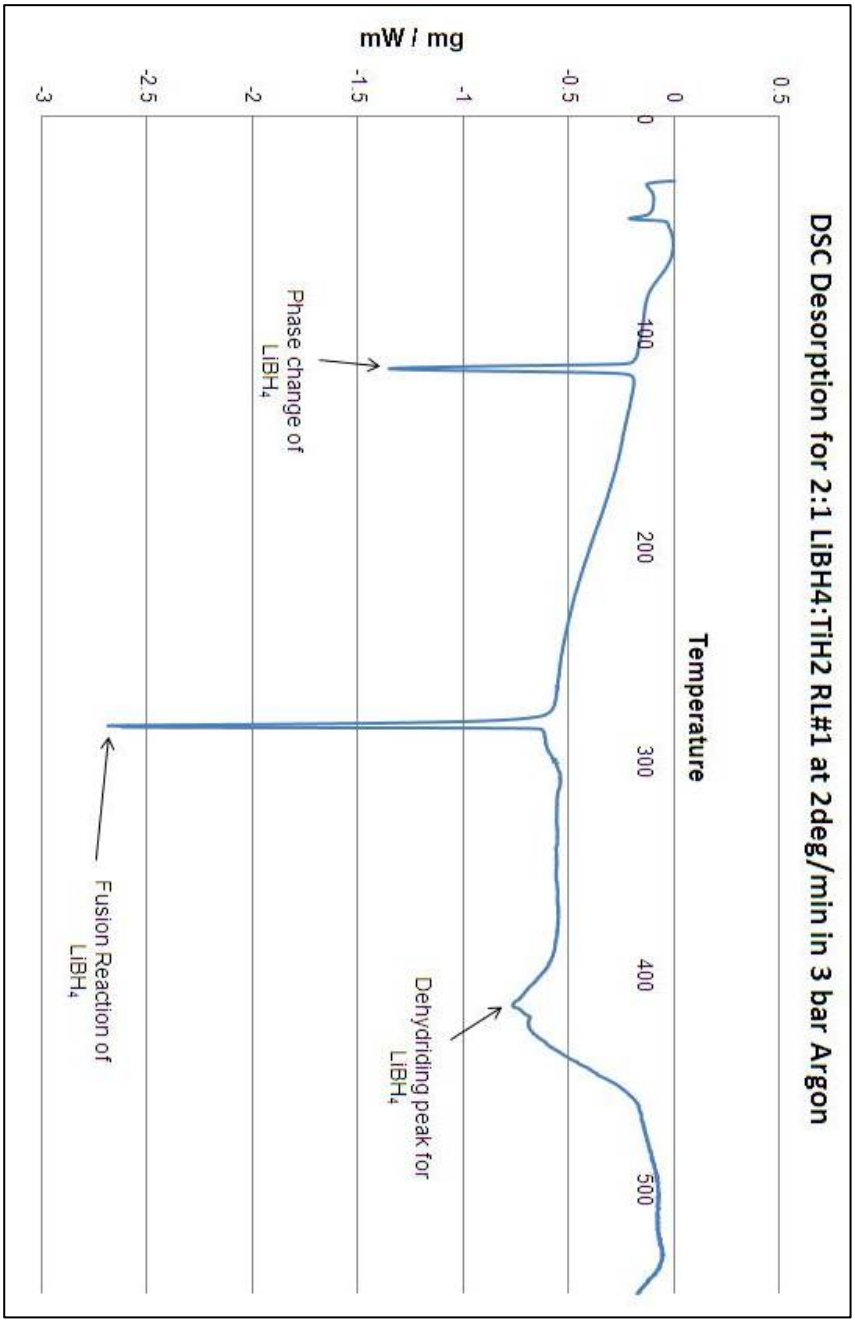

Figure 31 – DSC desorption profile for 2:1 $LiBH_4$:TiH_2 roller milled sample RL1

The DSC profile in figure 31 identifies two large peaks at approximately 110°C and 280°C, this is consistent with previous c-DTA calculations from TGA analysis which identified the same peaks. The structural peak and fusion peaks had associated enthalpies of 1.6 kJ / mol and 2.1 kJ / mol respectively. The dehydriding reaction of $LiBH_4$ had an enthalpy of 2.9 kJ / mol associated with it.

Orimo et al determined similar endothermic peaks from DSC analysis of as received $LiBH_4$, shown by figure 32. [28] The peak around 110°C relates to the polymorphic transformation of $LiBH_4$, from an orthorhombic structure or a hexagonal structure, the peak at 280°C relates to the fusion reaction of $LiBH_4$, at which point the substance melts. [10] The enthalpy of the peaks described previously, are consistent with the results of Orimo et al [28]; this suggests the rehydriding of the $LiBH_4$ products may be extremely difficult.

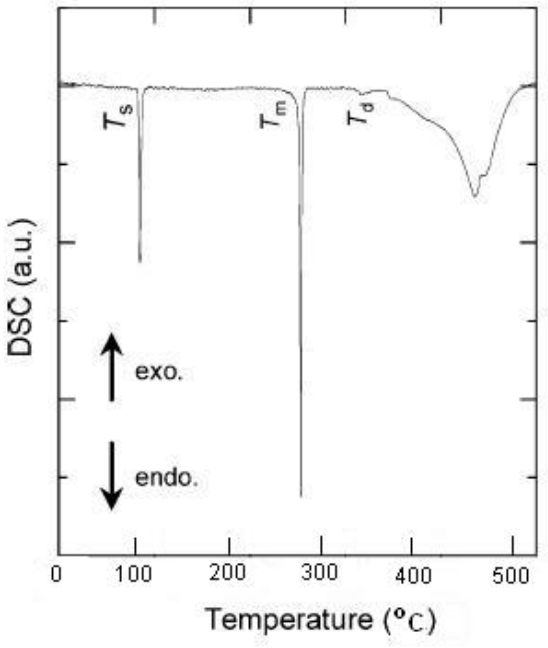

Figure 32 – DSC Profile of $LiBH_4$ heated at 10°C / min under 0.1 MPa of hydrogen[28]

The endothermic reaction shown in figure 31 beginning at approximately 420°C could be inferred to be due to the dehydriding reaction of $LiBH_4$. However, it occurs

approximately 30°C before the endothermic peak described by Orimo et al in figure 32 for as received $LiBH_4$, and has a significantly smaller enthalpy associated with it.

Yang et al determine that TiH_2 kinetically improves the desorption of $LiBH_4$, causing a modest reduction in desorption temperatures [14].

It could therefore be inferred that the major hydrogen desorption in the 2:1 $LiBH_4$: TiH_2 sample had already occurred, resulting in a much smaller peak relating to the dehydriding reaction of $LiBH_4$ occurring at approximately 420°C. This is consistent with previous TGA analysis in figure 30, where a major hydrogen desorption of approximately 4 wt% occurs after the fusion reaction at 280°C for sample RL1.

On observation of crimped DSC pan, a large percentage of the sample had bubbled through the hole in the lid and onto the DSC surface, the pot had also turned black. Although pan testing had confirmed that heating to 550°C was safe, it is possible the 3 bar atmosphere and longer heating time had caused the material to bubble out of the crimped pan. It was no longer considered safe to run the 2:1 $LiBH_4$: TiH_2 sample in the DSC without further examination of different pot materials and crimping techniques.

5.7 TPD Measurements (in HDDR rig)

TPD was carried out in a HDDR rig using the gas sorption system and loading techniques detailed in section 3.4. Using the gas sorption system it was determined that the volume of the furnace tube and connecting pipe work was 1.388 litres. Since a large proportion of this volume is contained within the furnace tube, it was necessary to calibrate the rig to allow for thermal gas expansion. The mass flow controllers were calibrated for hydrogen gas, and used to regulate the volume of gas flowing in and out of the system. This was pressurised to 1 bar hydrogen (a), the furnace tube was then heated to 600°C at its maximum heating rate of 10°C / min. 600°C was considered to be a high enough temperature to remove 13.5 wt% of the hydrogen from the $LiBH_4$; this was supported by Orimo et al who determined that only 4.5 wt% remained in the LiH product after heating using TGA analysis to 600°C, with 13.5 wt% of hydrogen being desorbed [10].

This measurement technique assumes that only H_2 is desorbed, however it is possible that very small amounts of other products may be desorbed, such as diborane. Since the HDDR rig output was not connected to a mass spectrometer, it was not possible to accurately characterise the gas desorbed, it is possible that a small amount of diborane may have formed.

Kostka et al examined the relative diborane concentrations from the desorption of as received $LiBH_4$ and mixed $LiBH_4$ composites, with additions such as silica gel and $TiCl_3$. [29] As received $LiBH_4$ produced no measurable diborane concentration upon desorption, however significant diborane concentrations were recorded for other mixed composites.

Kostka et al observed approximately 2 % relative concentration of diborane for an $LiBH_4$: SiO_2 gel milled composite when heated to 600°C. [29]

This is a concern, since in both the HDDR rig and microwave system, the samples will be contained in an SiO_2 test tube. However, Kostka et al milled the SiO_2 gel with $LiBH_4$, which would have resulted in a far larger surface of SiO_2 particles being in contact with $LiBH_4$ particles, than in the HDDR rig where only a small portion of the sample would be in contact with the SiO_2 test tube. Therefore it could be inferred that the relative concentration of diborane produced from $LiBH_4$ interaction with the SiO_2 test tube, would be significantly less than the 2 % relative concentration observed by Kostka et al when $LiBH_4$ was milled with SiO_2 gel.

Since TiH_2 is not expected to chemically react with $LiBH_4$, it would be reasonable to assume that the diborane produced from the $LiBH_4$: TiH_2 composites due to $LiBH_4$ desorption would be negligible. The bulk mass of gas within the system is inferred to be H_2, and any small volume of diborane present would be expected to have no significant effect on the volume reading. This is an advantage of a volumetric measurement; a gravimetric measurement may produce spurious results if even small amounts of diborane were produced.

The gas expansion due to heating inside the furnace tube, was recorded by the total gas passed out through mass flow controller 2, this is shown by figure 33.

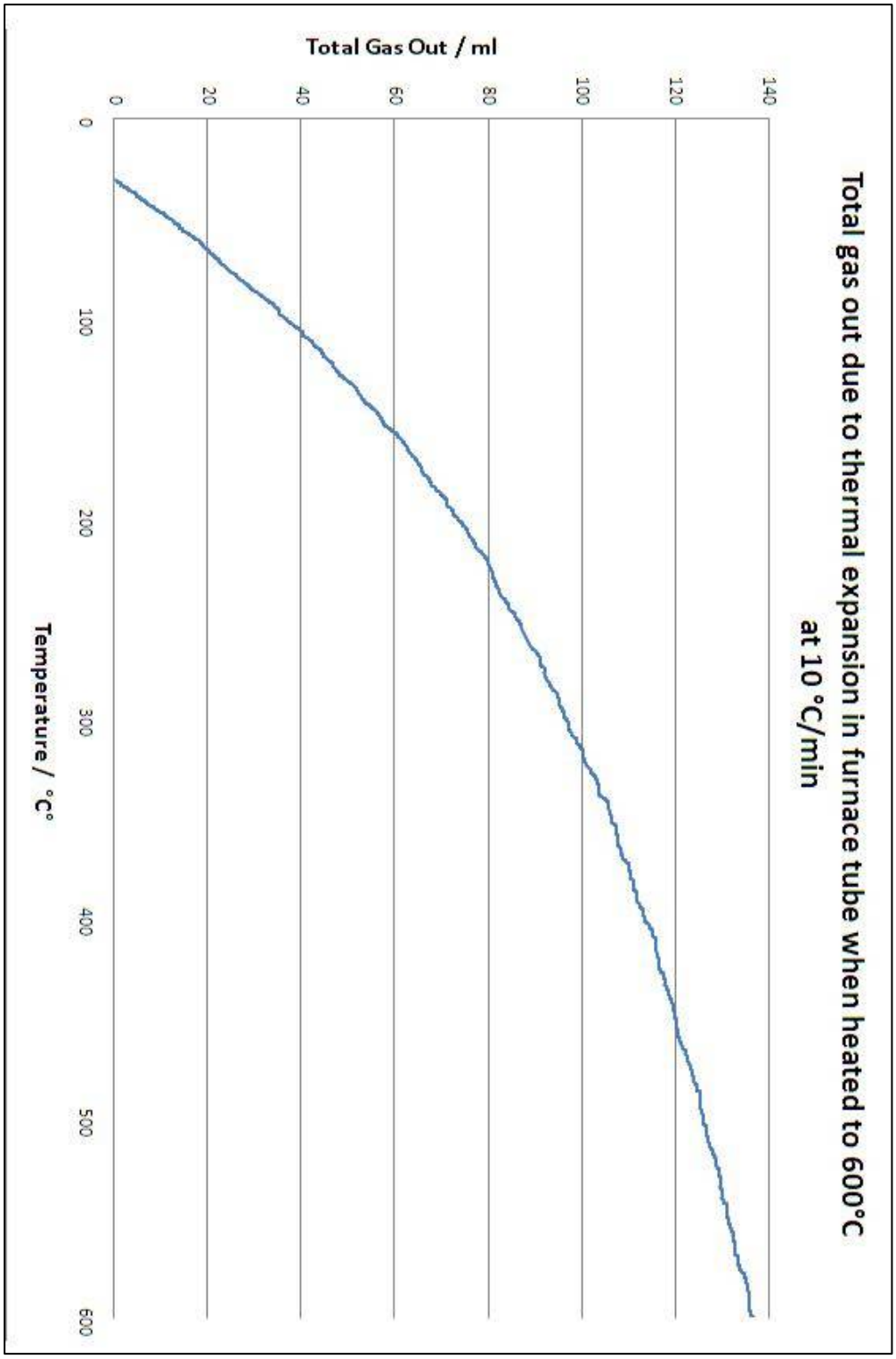

Since the calibration heating run was conducted at the same heating rate used to test the samples, it was possible to accurately match the temperatures of the calibration run and sample run and deduct the total gas out due to thermal expansion of hydrogen gas. For this

calibration and following measurements, time against temperature was linear throughout the heating range.

The samples were loaded into the test tube in an argon glovebox and transferred to the furnace tube inertly, the furnace was then heated at its maximum heating rate of 10°C / min to 600°C. Since the silica test tubes were considered to be single use items and the stainless steel furnace tube would be not be easily damaged by the sample bubbling over the top, the size of sample used in the HDDR experiments was able to be much larger than the size of samples used for DSC and TGA analysis. The sample size used in the HDDR experiments was approximately 500 mg, however, an even larger sample could have been used if necessary. This is in comparison to the small sample sizes of 5 mg or less used in TGA and DSC analysis.

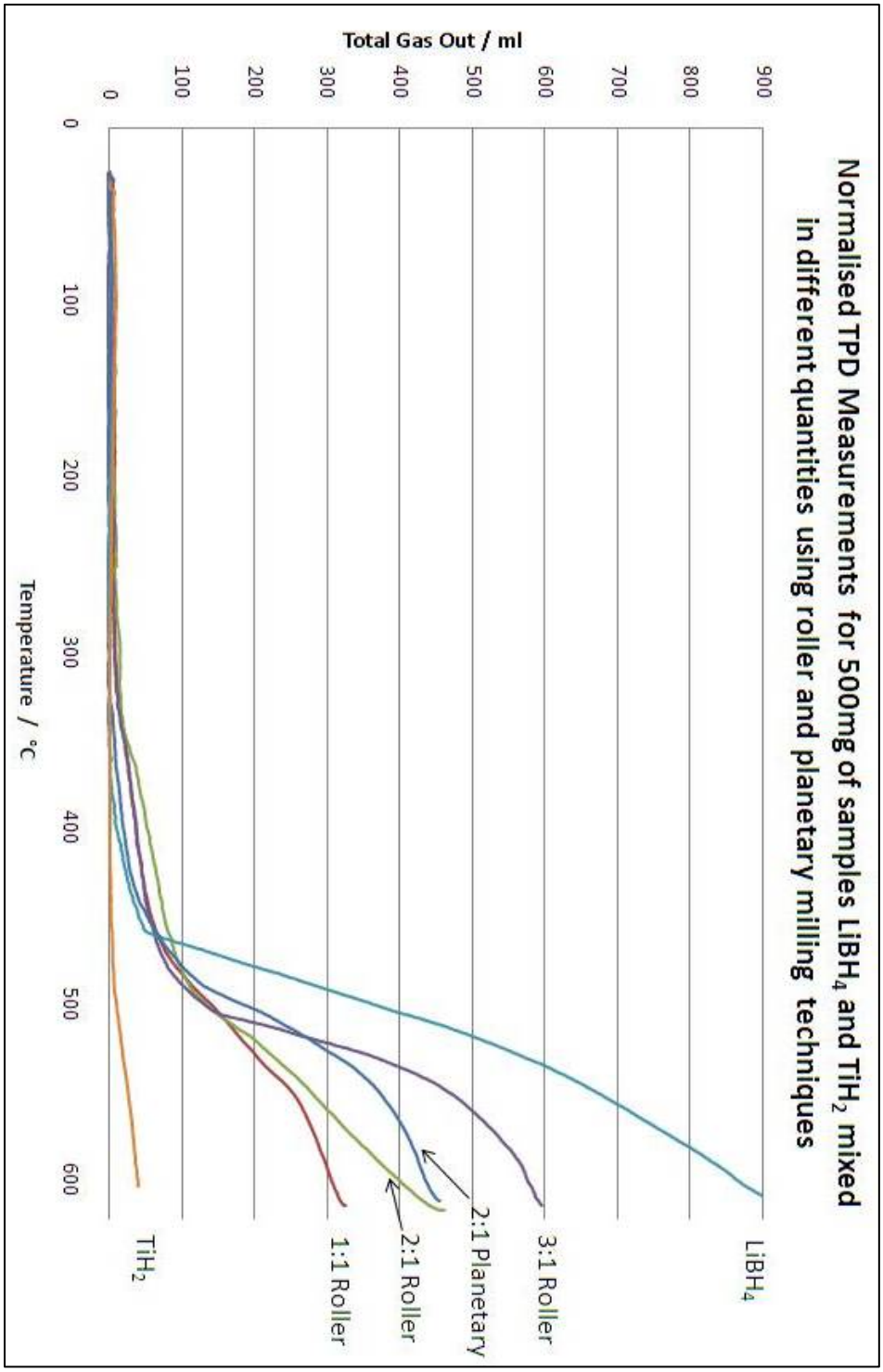

Figure 34 – TPD measurements in HDDR rig for starting materials and mixed composites heated to 600°C at 10°C /min

Figure 34 shows the volume of gas desorbed from the as received and composite samples. However, since the mass flow controllers record the volume of H_2 gas at STP, it is possible to determine the weight of the hydrogen gas desorbed, this can then be used to determine the % mass loss from the original sample.

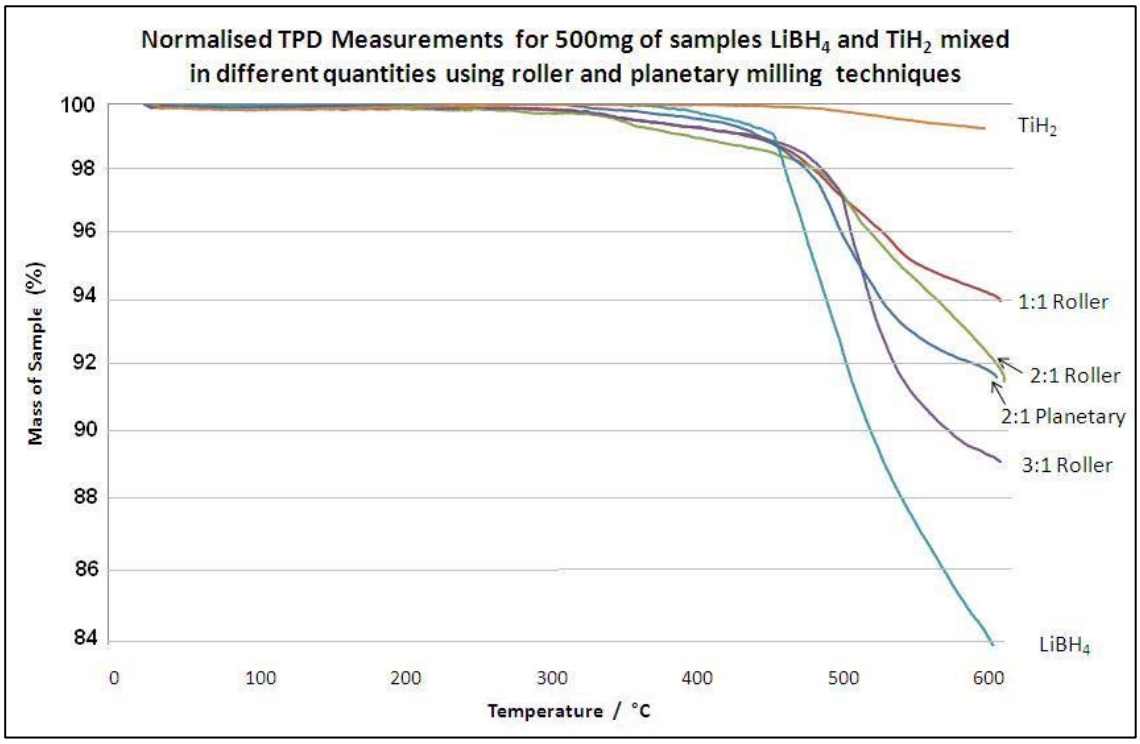

Figure 35 – TPD Measurements on as received and composite samples heated to 600°C at 10°C / min in the HDDR rig

Figure 36 – Desorption onset in as received and composite samples (figure 3x blown up)

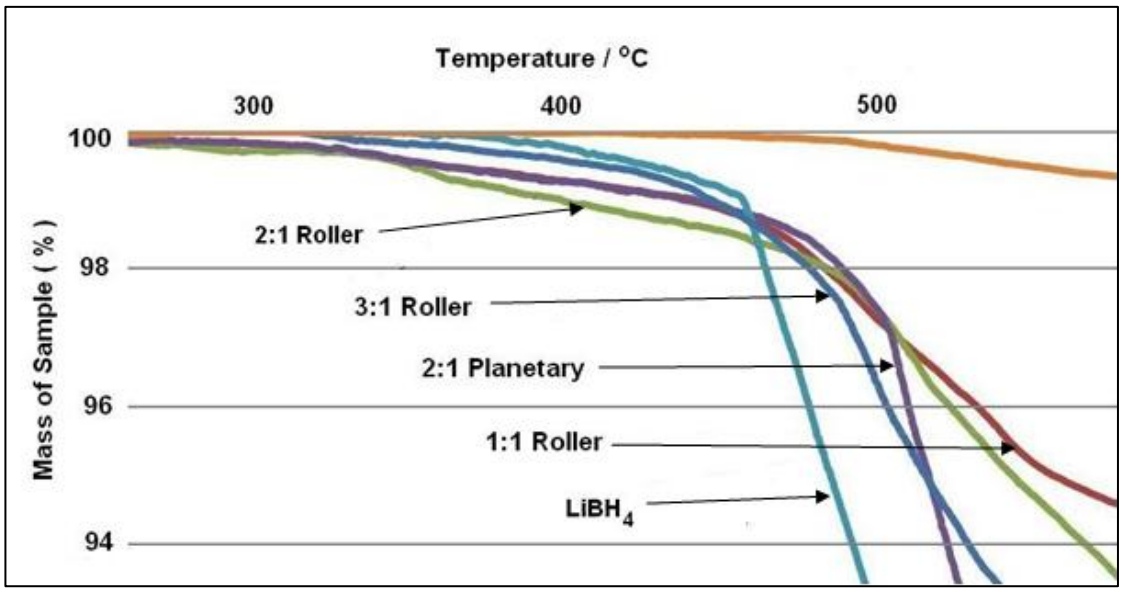

Figures 35 and 36 show the desorption characteristics of the various materials that were processed, by mass % of sample desorbed. All 2:1 and 1:1 $LiBH_4$: TiH_2 composites exhibited an initial hydrogen desorption beginning at 300°C to around 450°C, this was consistent with the onset temperature for the first hydrogen desorption in TGA analysis for the 2:1 $LiBH_4$:TiH_2 RL1 sample. Since these desorptions begin up to 50°C before the as received $LiBH_4$, it can be inferred that the addition of TiH_2 has

improved the kinetic properties of $LiBH_4$ effectively resulting in a reduction in desorption temperature, as documented by Yang et al. [14] The 3 : 1 $LiBH_4$:TiH_2 roller milled sample desorbed approximately 20°C later than the 2:1 and 1:1 composites at 320°C, it could be inferred that the smaller weight % of TiH_2 in the 500 mg sample improved the desorption kinetics of $LiBH_4$ by a lesser amount than the other composites.

Using TGA analysis, 4 wt% of the RL1 sample was desorbed between 300 - 400°C, in comparison to only around 1% for TPD measurements at this temperature. This may have been due to different atmospheric conditions, with 1 bar H_2 (a) present in the HDDR system, and 3 bar Ar (g) used for TGA analysis.

As received $LiBH_4$ began to desorb around 350°C, its major hydrogen desorption then began around 450°C, approximately 20°C before the milled composites. $LiBH_4$ continued to desorb hydrogen until 600°C, with the sample losing approximately 16 wt%. However, it is well documented that only a maximum of 13.8 wt% of hydrogen may be desorbed from $LiBH_4$ when heated to this temperature. The remaining 4.5% remains in the LiH desorption product which requires temperatures above its melting point of 680°C to desorb any hydrogen. [10]

Since the HDDR system maintains a constant pressure of 1 bar hydrogen (a), it is calibrated for gas expansion due to thermal heating. However, since a significant amount of hydrogen is being desorbed from the sample at high temperatures (in the order of 800 – 900 ml for a 500 mg sample of $LiBH_4$), the desorbed gas subsequently expands, pressuring the system further. This would then cause more hydrogen to be apparently removed from the system than had actually been desorbed from the sample, giving an inflated volume measurement.

To be able to calibrate the HDDR system for this desorbed gas expansion would be very difficult; gas is desorbed from the $LiBH_4$ and $LiBH_4$ composites at varying

temperatures over the heating range. To account for this, it would have been more beneficial to isolate the heating chamber from the gas sorption system while heating occurred, then to remove the total amount of gas above 1 bar pressure (a) once the heating chamber had cooled to room temperature. This would have enabled an absolute measurement of wt% desorbed from the composites due to hydrogen desorption. However, this methodology may have also caused problems due to the pressurisation of the system at high temperatures, although smaller sample size could have been used.

Although the HDDR system has been found to produce slightly inflated volume readings, it is still possible to use the HDDR results as a relative measure. When heated, as received TiH_2 exhibited a small hydrogen desorption starting at approximately 420°C where only 1 wt% mass was desorbed as hydrogen from a 500mg sample. This provides further evidence that TiH_2 is not a viable hydrogen store and should only be considered a susceptor material in the microwave project.

It was interesting to note that, the larger the amount of $LiBH_4$ contained within the composite, the sharper the hydrogen desorption peak. As received $LiBH_4$ exhibited the sharpest peak, desorbing approximately 900 ml of hydrogen for a 500mg sample, 1:1 $LiBH_4$:TiH_2 exhibited the smallest peak desorbing only 320ml of hydrogen gas.

Both samples RL1 and PL1 used a 2:1 ratio of $LiBH_4$:TiH_2, however the planetary milled substance desorbed slightly faster than the roller milled material over the complete temperature range. TiH_2 did not desorb a significant amount of hydrogen at 480°C. It could be inferred that the more finely distributed particles of the planetary milled composite allowed for a greater interaction of the $LiBH_4$ and TiH_4 particles, therefore a faster desorption of the $LiBH_4$ occurred due to more consistent heating throughout the material.

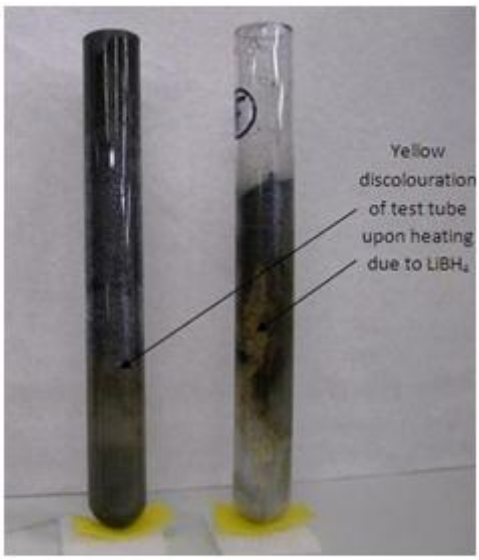

Figure 37 – Test tube discolouration after reaction with $LiBH_4$ upon heating

When heated in the HDDR, TiH_2 did not react with, or damage, the glass tubes. However, as shown in figure 37, $LiBH_4$ and the $LiBH_4$ composites caused significant damage to the test tubes rendering them useless after one sample run. Often the test tubes were completely cracked at the bottom and had failed; the samples frequently boiled over the top of the test tube when molar ratios of 2:1 $LiBH_4$: TiH_2 and greater were used.

This was a serious concern since the tubes used in the HDDR rig were the same tubes that would be used in the microwave system. These are the same effects which were observed during DSC and TGA pan testing, but on a larger scale.

It was decided that smaller samples would be used inside the test tubes for the microwave system, since if failure occurred the sample could boil through the inner and outer test tube and release hydrogen into the atmosphere.

5.8 XRD Analysis of Samples Run in HDDR Rig

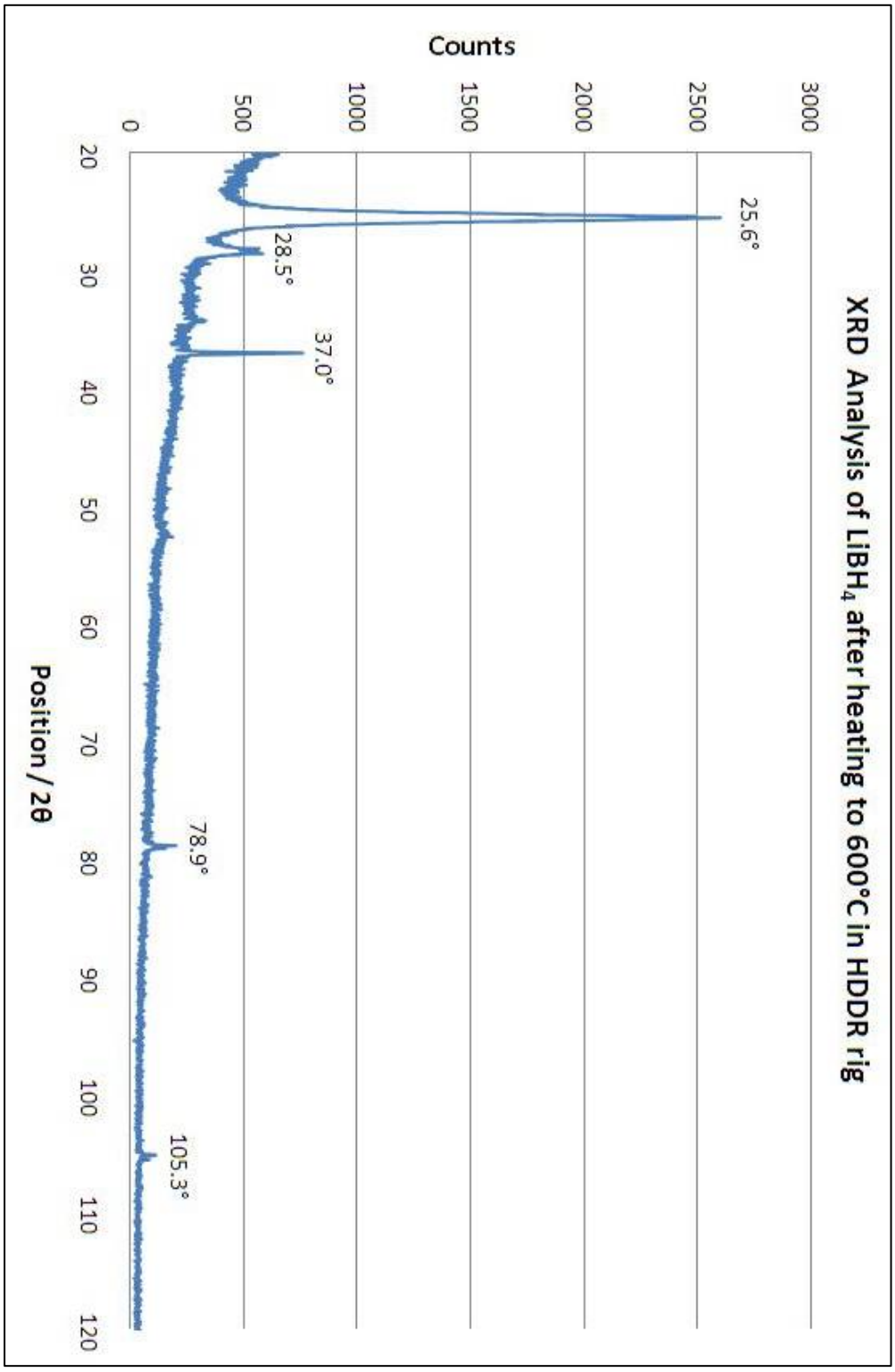

Figure 38 – XRD Analysis of $LiBH_4$ after being heated to 600°C in the HDDR rig

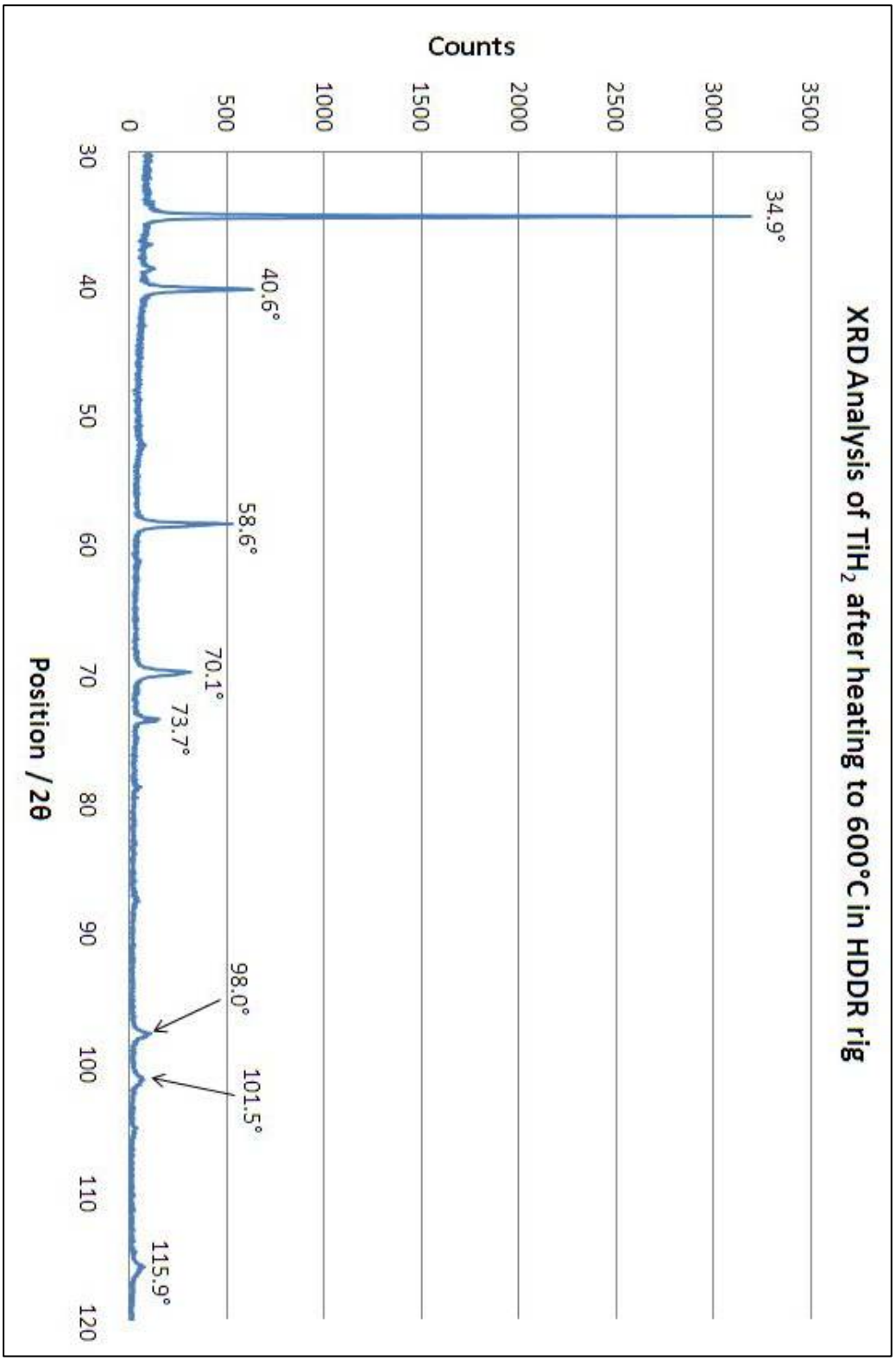

Figure 39 – XRD Analysis of TiH_2 after being heated to 600°C in the HDDR rig

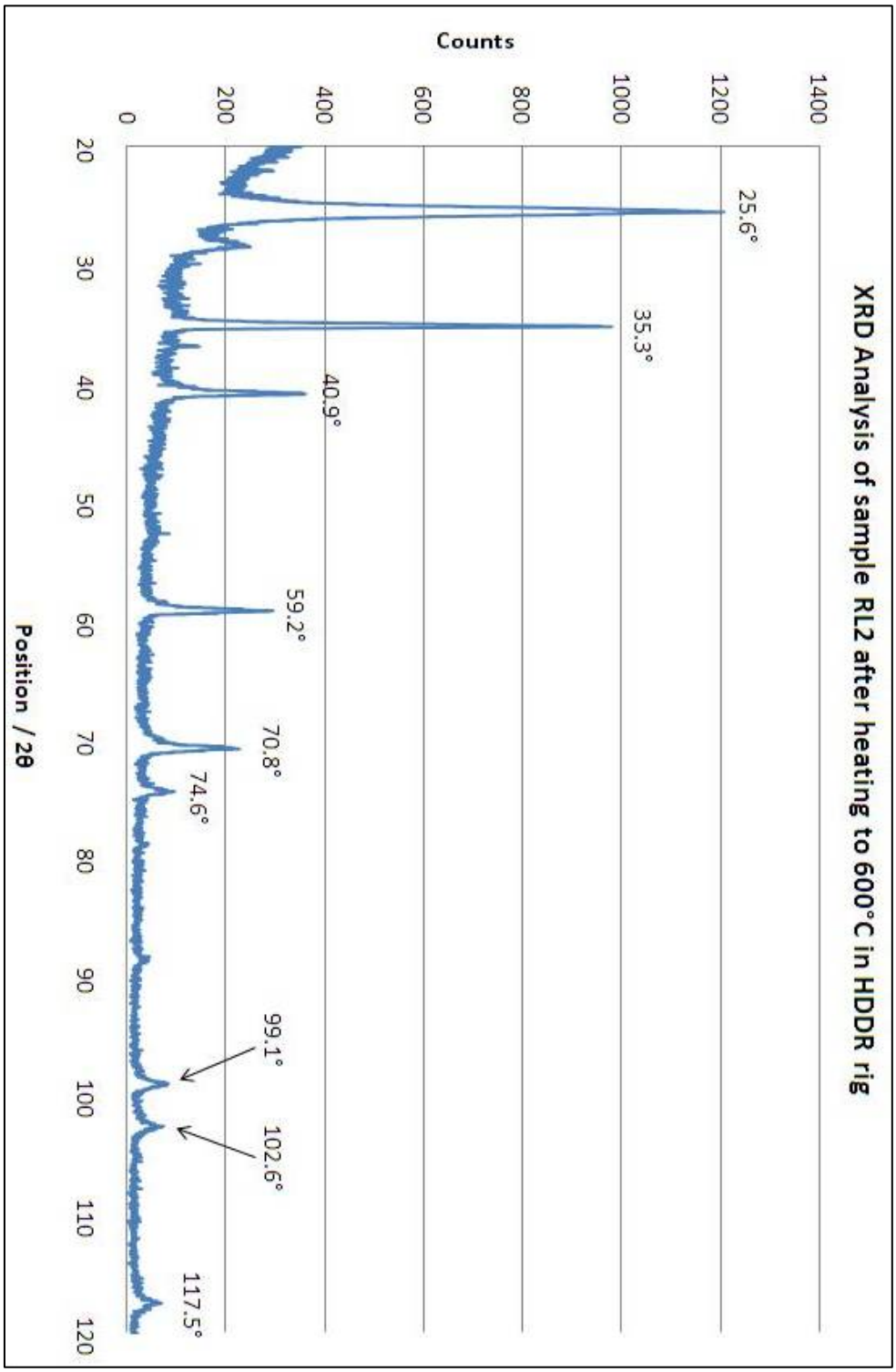

Figure 40 – XRD Analysis of RL2 (1:1 $LiBH_4$:TiH_2) after being heated to 600°C in the HDDR rig

Figure 40 shows the removal of the several significant $LiBH_4$ peaks such as 24.7° of 2θ, which represents the major peak for $LiBH_4$ in its orthorhombic structure. However, no peaks for LiH were observed, which is the supposed desorption product of $LiBH_4$; this may have been due to low scattering power of LiH due to the lightness of both ions. Bosenberg et al also had difficulties in identifying peaks for LiH upon desorption of $LiBH_4$ composites, it was concluded that this may be due to the small crystalline size of LiH upon heating. [30]

The XRD pattern in figure 39, for TiH_2 after HDDR analysis is virtually unchanged in comparison to the as received TiH_2 XRD spectra. Since only 1 wt% or less of TiH_2 was desorbed as hydrogen during HDDR analysis, it is likely that a large amount of TiH_2 remained within the XRD sample.

Bhosle et al determined, that TiH_2 changes phases from $TiH_2 \rightarrow TiH_x \rightarrow$ α-Ti between 0 and 700°C, where x is dependent upon particle size; the TiH_x phase is unstable at room temperatures and changes phase upon cooling to a mixed phase of (TiH_2 – α –Ti). This is consistent with figure 39, which exhibits no significant peaks for the TiH_x phase, where x = 1.92 – 0.7. However, no significant peaks for Ti were observed either; this may have been due to the very small of Ti which would have been present due to only 1 wt% of sample desorbed as hydrogen.

Sample RL2 again shows characteristics of both heated $LiBH_4$ and TiH_2 XRD spectra, with no new peaks being observed. Therefore it can be inferred that no significant reaction occurred between the two materials.

5.9 Microwave Analysis

5.9.1 Microwave Irradiation of TiH_2

Since TiH_2 was to be used as a microwave susceptor, it was important to determine how fast the material would be heated due to microwave irradiation at varying power intervals. A sample of 894 mg was loaded into the microwave tube inertly as detailed in the experimental section 4.4.1. In this experiment and all other microwave experiments, 100ml of de-ionised water of known di-electric loss was placed in a conical flask at the bottom of the microwave appliance detailed in the experimental section 4.5. The volume of the of microwave tube and connecting pipe work was 113 ml; this was much smaller than the HDDR rig which had a volume of 1.388 litres.

Since microwave irradiation can cause rapid localised heating of the sample and surrounding atmosphere, there was a significant risk that the glassware could melt; therefore a constant flow of 50 ml / min was passed through the microwave system to remove the desorbed hydrogen as quickly as possible. The volume of H_2 gas due to desorption could then be evaluated by accounting for this flow rate and measuring the volume of the increased flow due to hydrogen desorption from the sample.

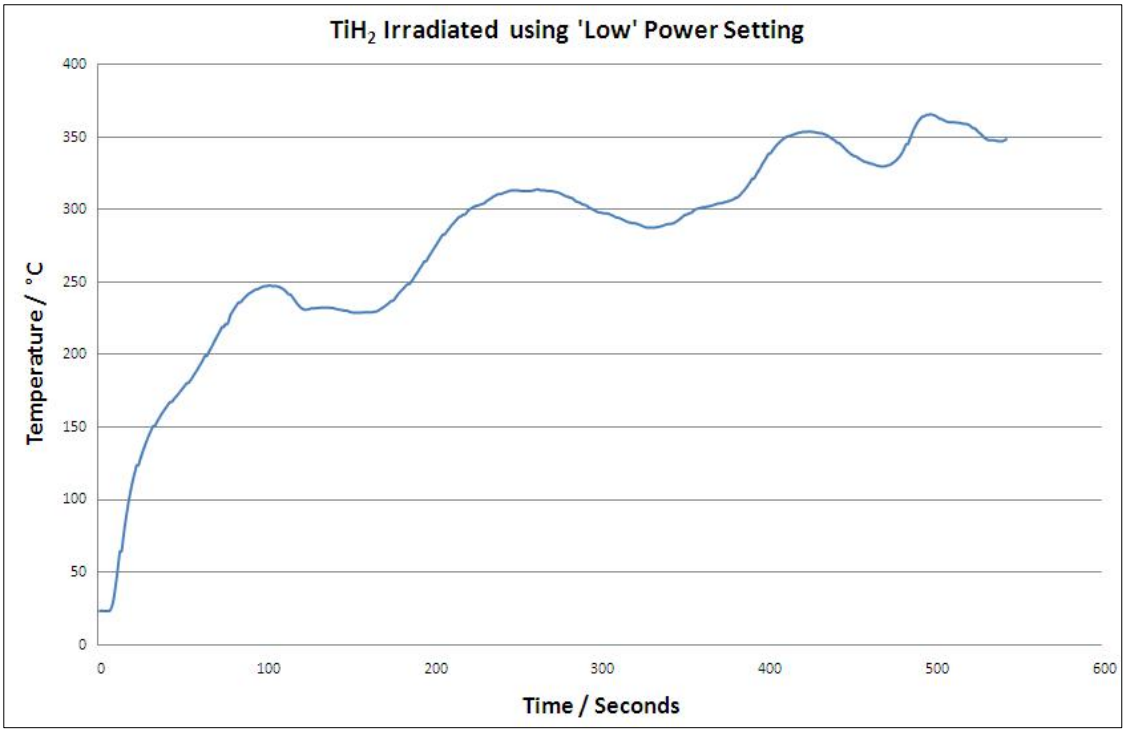

Figure 41 – Microwave irradiation of TiH_2 on 'low' power setting

TiH_2 was irradiated for 550 seconds and then switched off to prevent damage to the electrical wiring inside the microwave appliance. No measureable hydrogen desorption occurred due to microwave heating of the TiH_2 material. It was therefore concluded that a higher powered microwave mode may be required.

Although the microwave appliance was an "inverter" also detailed in the section 4.5, heating still appeared to occur in cycles. Since a mode stirrer was used inside the microwave appliance in an attempt to randomise the electromagnetic field it is possible that a "hot spot" was created when the mode stirrer was at a certain location within the field, causing the material to heat rapidly.

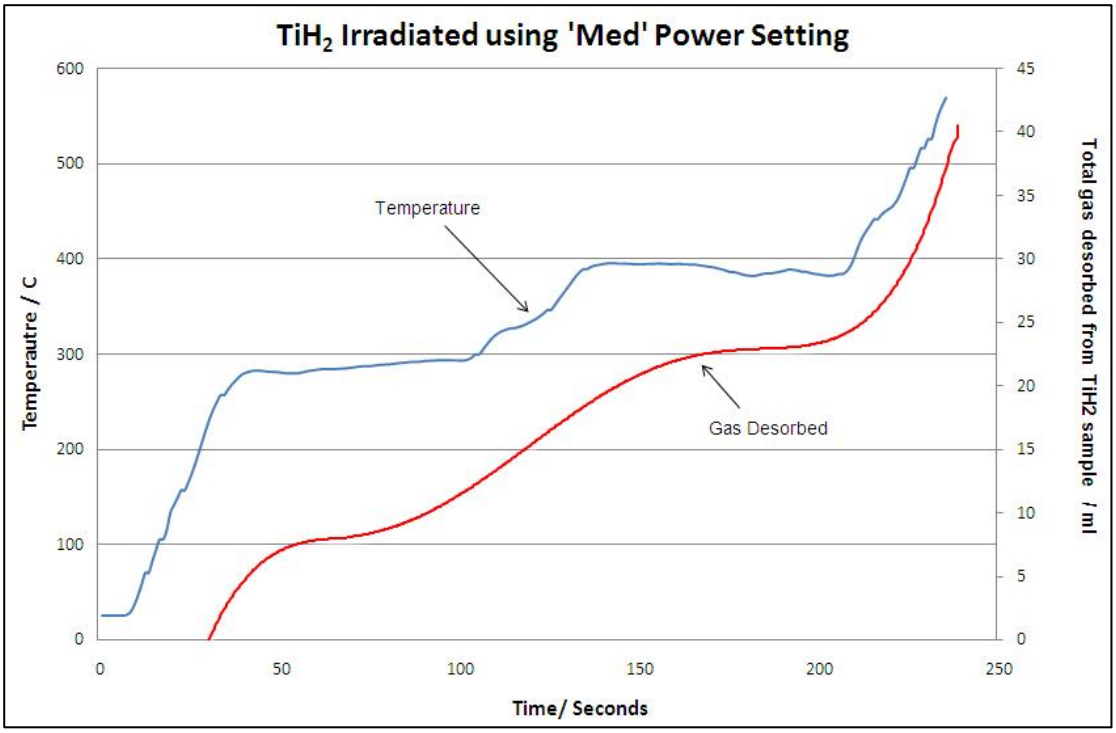

Figure 42 – Microwave irradiation of TiH_2 on 'med' power setting

In figure 42, TiH_2 was then cooled to room temperature and irradiated using the 'med' power setting. Since the microwave power had doubled, heating occurred at a much faster rate reaching 280°C in 40 seconds. The cycling heating effect observed in the low power irradiation, was also observed throughout medium power irradiation. After 240 seconds of irradiation the TiH_2 sample reached 580°C. The microwave appliance was then turned off.

The amount of H_2 gas desorbed from the TiH_2 sample relates to a mass loss of 0.4 wt%. This is significantly less than was observed through HDDR analysis of as received TiH_2 powder when heated to 600°C, with approximately 1 wt% of the sample being desorbed as hydrogen. Orimo et al observed similar results when heating as received TiH_2 powder using microwave irradiation, with less than 0.16 wt% of the TiH_2 sample being desorbed as hydrogen. [24] Orimo et al concluded that this was due to the

microwave penetration depth being significantly smaller than the TiH_2 particle size. The slightly larger wt% of TiH_2 desorbed in figure 42 may have been due to the temperature of the TiH_2 powder reaching 550°C where desorption may have occurred through conductive heating. This is in comparison to Orimo et al who observed heating of TiH_2 to only 375°C. [24]

Microwave irradiation of as received TiH_2 caused steep heating rates which potentially offers large savings in energy in comparison to conventional TPD heating. However it would have been useful to examine the microwave irradiation of milled TiH_2 powder to determine if the decrease in particle size (in the order of size of the microwave penetration depth) allowed for greater hydrogen desorption to occur.

TiH_2 acted as a suitable susceptor material exhibiting rapid temperature increases, it was therefore assumed that it would aid hydrogen desorption from $LiBH_4$ in $LiBH_4$: TiH_2 composites through conductive heating, under microwave irradiation.

5.9.2 Microwave Irradiation of $LiBH_4$ Composites

The first composite to be investigated for irradiation was the 2:1 $LiBH_4$: TiH_2 RL1 sample. 145 mg of the sample was inertly loaded in an argon glovebox and irradiated for 10 minutes on the ‘medium’ power setting.

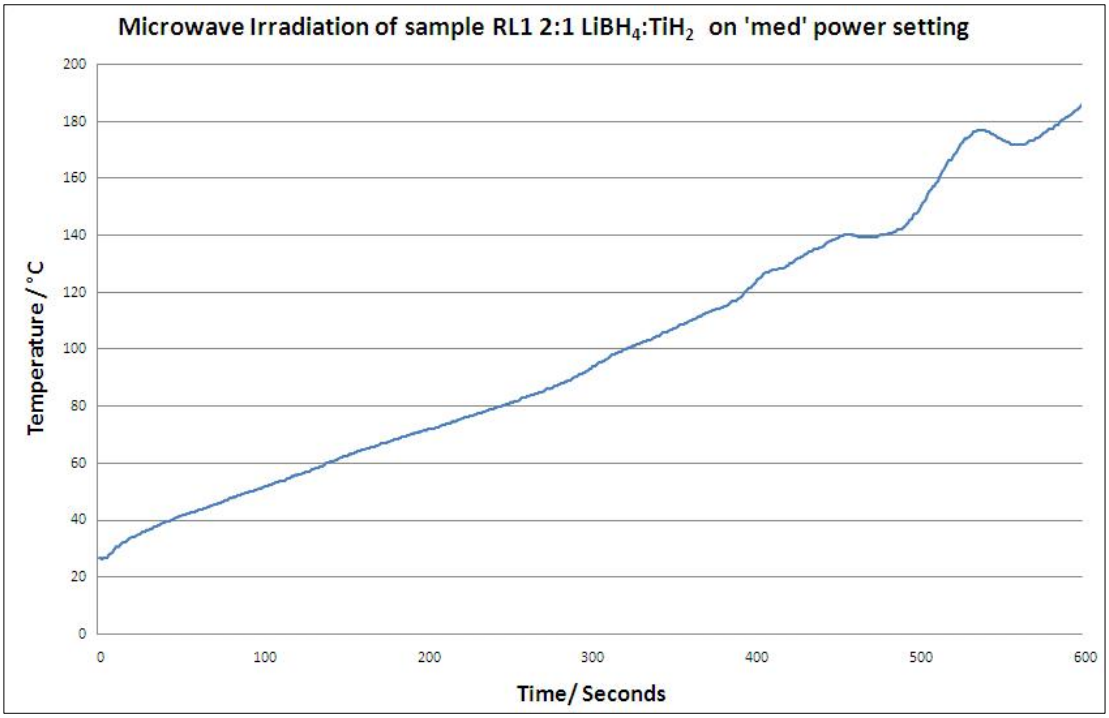

Figure 43 – Microwave irradiation of 2:1 $LiBH_4$:TiH_2 RL1 on 'medium' power setting

Figure 43 shows that after 10 minutes, the $LiBH_4$ composite only reached 183°C at which time the microwave appliance was turned off to protect the internal wiring from overheating. This was a relatively small increase in temperature when compared with the heating of TiH_2 which reached 580°C in only 240 seconds when under microwave irradiation, on the 'medium' power setting.

There was no significant measureable desorption of hydrogen gas from the 2:1 RL1 sample. This was consistent with microwave measurements for TiH_2, which only produced a measurable hydrogen desorption after reaching a temperature of above 200°C, shown in figure 42. Orimo et al did observe a small hydrogen desorption from a 2:1 $LiBH_4$: TiH_2 composite before 200°C [24]. However this was not observed in the initial microwave measurement for the RL1 sample on the 'medium' powder setting, so it was determined that a higher microwave power setting may be required.

Once again a slight heating cycle effect was observed towards the end of irradiation, since this was not present throughout the rest of the experiment, it is possible that the microwave transmitter was automatically turned off when the internal wiring began to overheat.

The 145 mg sample was left to cool to room temperature and then irradiated using the 'max' power setting, since the 'medium' power setting was not sufficient to cause desorption in the powder after 10 minutes of irradiation.

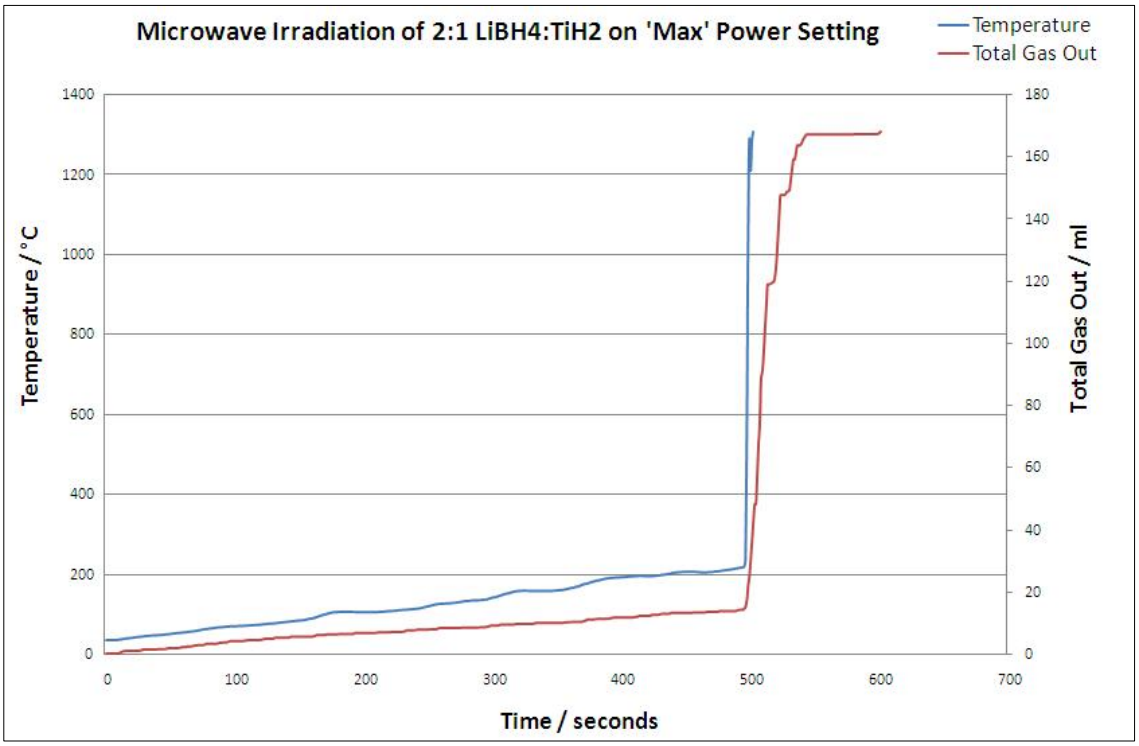

Figure 44 – Microwave irradiation 2:1 $LiBH_4$:TiH_2 on 'high' power setting

Figure 44 shows the RL1 sample increased uniformly in temperature to approximately 210°C due to microwave irradiation. However at this point a rapid increase in temperature and gas desorption was observed, the material heated from 210°C to

1309°C in only 6 seconds, this melted the inner test tube. At this point the experiment was terminated and the microwave system was turned off.

In total, a volume of 165 ml of H_2 was desorbed from the RL1 composite, this equates to a 9.80 wt% mass loss from the sample. Since the temperature reached above 1300°C, it is feasible that not only did the $LiBH_4$ desorb hydrogen as described by equation (1) producing a LiH desorption product, but the LiH itself decomposed to release hydrogen, which occurs above its melting temperature of 680°C [9]. TiH_2 also desorbs approximately 3.5 wt% of hydrogen when heated to 600°C, as described by Bhosle et al [13]. If all the hydrogen was to be desorbed from the $LiBH_4$: TiH_2 composite, the sample would have lost 10.77 wt% upon heating, which is in the same order as the 9.80 wt% loss in sample mass of RL1 in figure 43.

It is unclear why such a rapid heating occurred at this temperature, a structural change does occur in $LiBH_4$ at 120°C at which point the dielectric properties of the material become more favourable for microwave absorption, the dielectric constant and loss factor rising from 5 to 20 and almost 0 to 5 at this point respectively. However, Orimo et al observed that the rapid heating of the $LiBH_4$: TiH_2 occurs at a higher temperature closer to the fusion reaction in $LiBH_4$ at 280°C. Orimo et al observed a 275°C increase in sample temperature at this point, within 1 minute. [23].

The K-thermocouple was placed as close as possible to the sample material in the microwave sample tube, however it would have not been able to measure temperature increases in very localised areas in the centre of the sample. Microwaves have ‘hot spots’ which can be in the order of nanometres wide; some parts of the $LiBH_4$ may have therefore undergone the fusion reaction and be at a much higher temperature than other parts of the powder; this would allow for greater microwave absorption in

these areas, as observed by Orimo et al's study of the di-electric properties of $LiBH_4$. [24]

It is also possible that the fusion reaction, where $LiBH_4$ had melted, could have caused a catalytic reaction with the glassware as the test tube melted, causing the temperature to rise rapidly. Zuttel et al observed significantly faster desorption rates in $LiBH_4$ milled with SiO_2 powder, the onset temperature for hydrogen desorption was approximately 220°C [10], which is consistent with the hydrogen desorption onset temperature observed in figure 43 when the $LiBH_4$: TiH_2 was heated through microwave irradiation.

On examination of the glassware, the silica test tube had melted at the bottom and completely failed, there were also large cracks throughout the upper part of the tube. The greatest concern was that the outer glassware had also cracked due to the sudden large change in temperature, if this had completely failed, hydrogen would have been pumped into the room. It should be noted that there are hydrogen detectors in the laboratory which would subsequently sound an alarm and turn the hydrogen supply off.

It was important to examine the point at which the temperature increased rapidly. Since the irradiation of TiH_2 was relatively uniform in comparison, the 1:1 $LiBH_4$: TiH_2 RL2 sample was chosen since it had a larger amount of TiH_2 in the composite. To try and reduce the sudden change in temperature of the glassware, the sample and microwave test tubes were gently heated with a hot air gun to 120°C after an 80 mg sample had been inertly loaded in an argon glovebox.

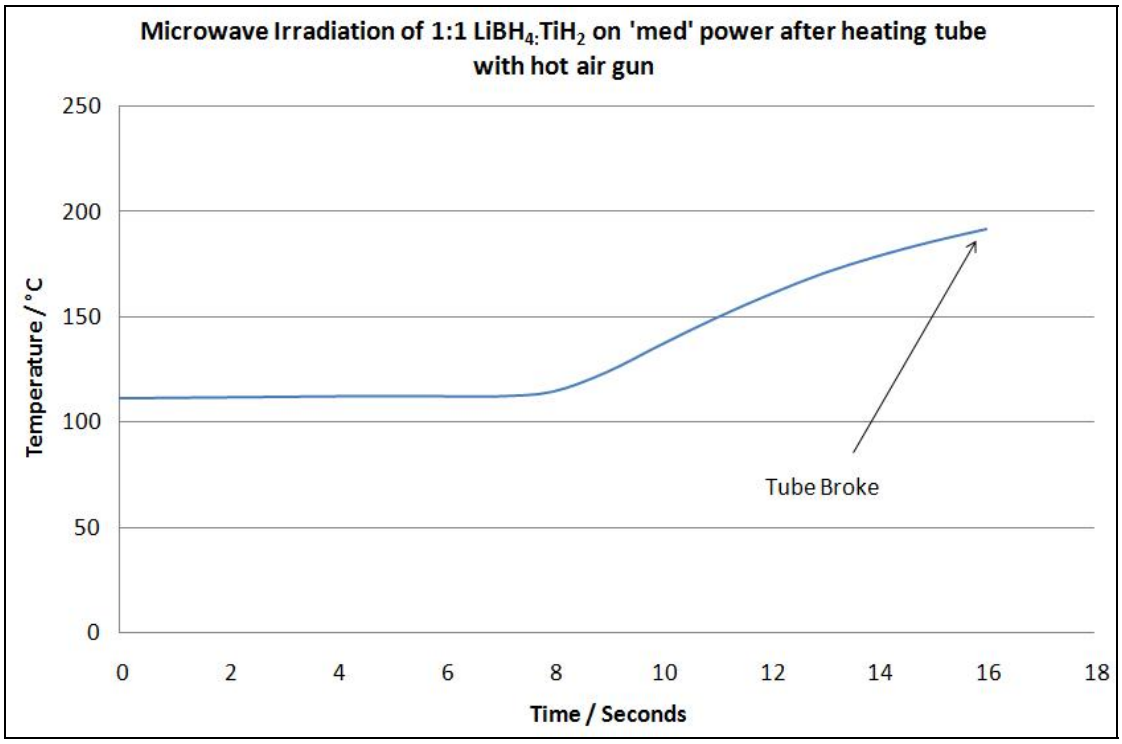

Figure 45 – Microwave irradiation of 1:1 $LiBH_4$:TiH_2 RL2 on 'medium' power setting after heating with hot air gun

Figure 45 shows that after only 10 seconds of microwave irradiation, the inner silica tube failed. It could be inferred that this was due to a large increase in temperature of the powder, however it cannot be confirmed since the tube broke before the thermocouple was able to measure the temperature increase and dropped the bottom of the outer test tube shown in figure 46.

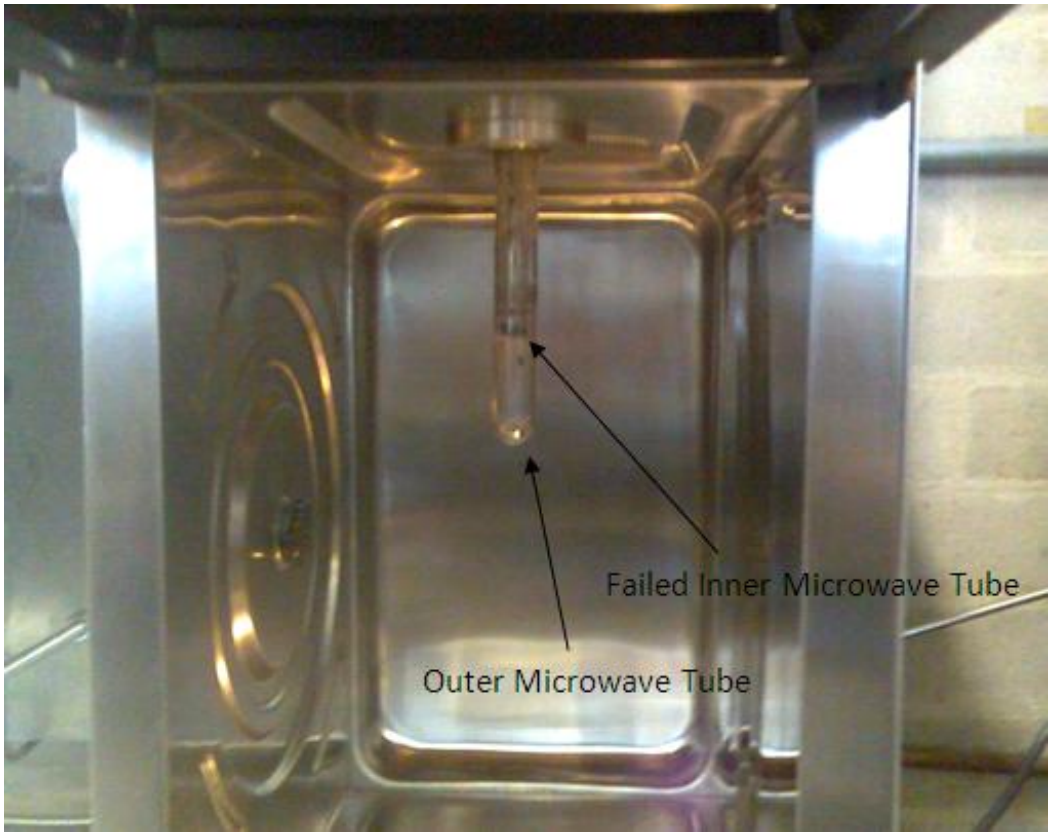

Figure 46 – Inside the microwave cavity after inner test tube had failed

The failing of the inner microwave tube was a serious issue, but the major concern was the cracking of the outer microwave tube. If this was to be replaced, the outer silica tubes were costly and had to be welded to the metal clamp at the top of the tube which was a very time consuming process. During each microwave experiment a crack would either form or propagate causing the outside tube to weaken, this was a serious safety concern, since if the outer tube had failed, the mass flow controllers would have attempted to maintain the atmosphere at 1 bar. This would have pumped hydrogen into the room until a detector turned off the supply.

Another serious problem was the loading of the inner test tube in the argon glovebox. The silica hooks which hung the inner test tube from the thermocouple casing were

difficult to manufacture and easily broke upon loading. Due to the loading difficulties and the consistent weakening of the outer-tube, further experiments were not successful. It was therefore not possible to exactly determine what effect had occurred to cause such a major temperature rise in the 2:1 $LiBH_4$: TiH_2 sample.

It was also not possible to analyse the samples using X-ray diffraction after microwave irradiation, since only a fine layer of sample was left on the silica test tube which could not be scraped off. However, it may have been possible to break off part of the test tube for IR and Raman spectroscopy analysis, to study the vibrational and rotational modes of the desorption product.

Orimo et al examined the microwave irradiation of $LiBH_4$: TiH_2 composites, and other $LiBH_4$ doped materials. However the methodology is significantly different to that examined in this thesis. Orimo et al contain the composites in a Teflon container, measuring the temperature and pressure using a K-type thermocouple and pressure gauge, the container is loaded inertly and isolated from the outside atmosphere during irradiation. [24] This methodology removes many of the problems examined using the gas sorption system, including difficult loading techniques, damage to the silica test tube due to large heating rates, and reactions of the composite with the silica test tube surface.

It would be useful to continue the analysis of microwave induced desorption of lithium borohydride-based composites, particularly investigating the rapid temperature increase exhibited by the RL1 composite at 200°C. This rapid desorption of hydrogen gas would be of particular use in a hydrogen store where energy is often required quickly, it would be useful to investigate what microwave effects are occurring to cause such a rapid increase in temperature so that the full advantages of a microwave system can be utilised, this would allow for a much more effective solid state hydrogen store.

Although it was not possible to absolutely characterise the energy differences between microwave irradiation and conventional heating, it is clear from the measurements made on both the HDDR rig and microwave system, that microwave irradiation is able to deliver significantly increased heating rates potentially offering significant energy savings compared with conventional heating techniques. This is widely documented throughout many microwave papers; Thostenson et al conclude that large energy savings are made due to direct molecular interaction with the electromagnetic field meaning that heating does not rely on diffusion of heat from the surfaces. [19]

Comparison of TGA analysis in figure 29 and microwave induced desorption analysis in figure 43 highlight the differences in desorption kinetics and energy requirements of the two heating techniques. Desorption observed in TGA analysis was over many minutes, in which less than 5 wt% of the sample was desorbed as hydrogen, this also incurred large energy losses due to the heating of the TGA furnace, with much of the energy wasted.

This is in comparison to microwave induced desorption in which the sample desorbed almost all the hydrogen (9.80 wt%) in the $LiBH_4$: TiH_2 composite due to a very large temperature increase of over 1200°C in less than 10 seconds. Although it required many minutes of microwave irradiation to produce such a rapid desorption, the introduction of more efficient catalysts and susceptor materials would reduce the energy requirements of microwave heating further. It would be almost impossible to replicate these heating rates and desorption kinetics using conventional heating techniques.

6. Conclusions

The thesis is partially successful in making a comparison between conventional heating methods and microwave irradiation. There were many difficulties in comparing the techniques, such as the differences between gravimetric and volumetric measurements.

XRD data identified the starting materials $LiBH_4$ and TiH_2. After TPD heating, the decomposition product of $LiBH_4$, LiH was not characterised. This was determined to be due to the lightless of the ions in the hydride, however it can be inferred that hydrogen was desorbed from the $LiBH_4$ under TPD heating due to the measurement made by the mass flow controllers. SEM pictures were taken of the starting materials and milled composites; this data seemed to contradict the XRD analysis in which $LiBH_4$ exhibited broader peaks. SEM-EDS should have been performed on all the materials to identify the compounds present so further analysis could be made.

The volatility of $LiBH_4$ made DSC and TGA measurements hazardous to the respective instruments particularly at high temperatures and only limited data was collected for these techniques. However, when using the HDDR rig, this was not an issue and a full set of data for all starting materials and milled composites was collected. Although the volumetric measurement was not considered to be absolutely accurate (due to the offset from hydrogen expansion), it did accurately characterise the differences in hydrogen desorption for the different compounds as expected from the literature review.

Microwave induced desorption of various composites on ‘high’ power produced much faster heating rates than were exhibited under TPD heating; hydrogen desorption also occurred much faster. It would have been beneficial to determine the power that was delivered to the sample using this technique, however, without further analysis or re-

designing to the system to have single-mode cavity, this was only able to be roughly determined.

On review of the data, even though it was not accurately characterised, it would seem that significant energy savings are available using microwave heating techniques. TiH_2 was found to kinetically destabilise the desorption of $LiBH_4$ in all techniques. For microwave irradiation it can be inferred that TiH_2 acted as a susceptor material thereby promoting desorption of hydrogen from the $LiBH_4$ and reduced the energy required to heat the composite.

7. Further Work

Although the microwave system was successful in producing rapid heating rates and improved desorption kinetics, difficulties in loading samples and damages to the silica test tubes significantly reduced its effectiveness. Other materials should certainly be considered to house the sample within the system, such as Al_2O_3, or Teflon, as used by Orimo et al. [24]

It would be useful to heat $LiBH_4$ composite samples to varying temperatures using both microwave and conventional heating techniques, so that XRD and Raman spectroscopy could be performed. This would enable a greater understanding of the intermediate phases of both $LiBH_4$ as examined by Orimo et al [31] and TiH_2 as examined by Bhosle et al [13], to more accurately characteristic the desorption profiles of both materials.

The effect of particle size of TiH_2 should be more thoroughly explored. Orimo et al determine that the TiH_2 particle size is significantly larger than the penetration depth of microwave irradiation [24] Bhosle et al determined that high energy mechanical milling of as received TiH_2 reduced particles sizes to 10nm or less [13], therefore, examining microwave irradiation of milled TiH_2 powder of different particle sizes may determine improved milling methodology to make TiH_2 a more effective susceptor in microwave experiments.

Various other additions to $LiBH_4$ should also be considered, such as C, B and SiO_2. C and B are known to be effective susceptor materials in microwave irradiation as determined by Orimo et al [26]. SiO_2 should also be considered, since it acted as an effective catalyst in conventional heating when doped with $LiBH_4$ as determined by Zuttel et al [7]; the increased heating rates exhibited in microwave irradiation may offer an even greater catalytic effect.

Since DSC / TGA analysis was widely unsuccessful due to the sample bubbling over the DSC pan and TGA pot, different materials should be considered to house the sample for this analysis, such as Pt and tantalum.

Re-absorption has only been briefly mentioned in this thesis. However, without a suitable re-absorption mechanism, $LiBH_4$ cannot be considered to be a viable hydrogen store. It would be highly beneficial to examine systems which could combine microwave irradiation desorption and re-absorption to produce a $LiBH_4$ based hydrogen store which could have favourable hydrogen desorption and re-absorption kinetics, with resistance to degradation from repeated cycling.

References

1. CIA World Factbook, World Population July 2008 est. Available at: https://www.cia.gov/library/publications/the-world-factbook/geos/xx.html#People Accessed on 29/09/2008
2. Energy Information Administration (EIA) – *International Energy Annual 2005 (June – October 2007),* Also Available at: http://www.eia.doe.gov/oiaf/ieo/highlights.html Accessed on 29/09/2008
3. Energy Information Administration (EIA) – *International Energy Outlook 2008* Available at: http://www.eia.doe.gov/oiaf/ieo/nat_gas.html Accessed on 29/09/2008
4. A. Zuttel and L. Schlapbach, *Nature*, **414**, 2001, pg. 353
5. A. Zuttel, P. Wenger, P. Sudan, P. Mauron and S. Orimo, *Materials Science and Engineering B*, **108**, 2004, pg. 9
6. S. Satyapal, J. Petrovic, C. Read, G. Thomas and G. Ordaz, *Catalysis Today*, **120**, 2007, pg. 246
7. A. Zuttel, S. Rentsch, P. Fischer, P. Wenger, P. Sudan, Ph. Mauron, Ch. Emmenegger, *Journal of Alloys and Compounds,* **356-357**, 2003, pg. 515-520
8. K. Miwa, N. Ohba, S. Towata, Y. Nakamori, S. Orimo, *Physical Review B,* **69**, 2004, pg. 245120
9. Y. Nakamori, A. Ninomiya, G. Kitahara, M. Aoki, T. Noritake, K. Miwa, Y.Kojima, S. Orimo, *Journal of Power Sources,* **155**, 2006, pg. 447-455
10. A. Zuttel, P. Wenger, S. Rentsch, P. Saudan, Ph. Mauron, Ch. Emmenegger, *Journal of Power Sources* **118**, 2003, pg 1-7

11. M. Au, A. Jurgensen, K. Zeigler, *Journal of Physical Chemistry B,* **110**, 2006, pg. 26482-26487
12. M. Au, A. Jurgensen, *Journal of Physical Chemistry B,* **110**, 2006, pg. 7062-7067
13. V. Bhosle, E. Baburaj, M. Miranova, K. Salama, *Materials and Engineering,* **356**, 2003, pg. 190-199
14. J. Yang, A. Sudik, C. Wolverton, *Journal of Physical Chemistry C,* **111,** *2006,* pg. 19134-19140
15. Electro Optical Industries – Electromagnetic Spectrum
    Available at: http://www.electro-optical.com/html/bb_rad/emspect.asp
    Accessed on 29/09/2008
16. H. Will, P. Scholz, B. Ondruschka, *Topics in Catalysis,* **29,** 2004, pg. 3-4
17. Y. Bykov, K. Rybakov, V. Semenov, *Journal of Physics D: Applied Physics* **34**, 2001, pg. 55-75
18. D. Clark, D. Folz, J.West, *Materials Science and Engineering*, **A287**, 2000, pg. 153-158
19. E. Thostenson, T. Chou, *Composites Part A,* **30**, 1999, pg. 1055-1071
20. Y. Nakamori, M.Matsou, K. Yamada, T. Tsutaoka, S. Orimo, *Journal of Alloys and Compounds,* 2007
21. CEM Corporation – Microwave Wave Function –
    Available at : http://www.cem.com/biosciences/mwbasics_pep.asp
    Accessed on 29/09/2008
22. AZoM – The "AZo Journal of Materials Online",
    Available at : http://www.azom.com/details.asp?ArticleID=937
    Accessed on 29/09/2008
23. G. Roussy, E. Marchale, J. Thiebaut, A. Kiennemann, *Fuel Processing Technology*, **50**, 1997, pg. 261

24. Y. Nakamori, S. Orimo, T. Tsutaoka, *Applied Physics Letters,* **88**, 2006, pg. 112104
25. Y. Nakamori, S. Orimo, T. Tsutaoka, M. Matsuo, K. Yamada, *Journal of Alloys and Compounds,* **446-447**, 2007, pg. 698-702
26. Y. Nakamori, S. Orimo, M. Matsuo, K. Yamada, *Applied Physics Letters,* **90**, 2007, pg. 232907
27. C. Suryanarayana, *Progress in Materials Science*, **46**, 2001, pg. 1-184
28. S. Orimo, Y. Nakamori, G. Kitahara, K. Miwa, N. Ohba, S. Towata, A. Zuttel, *Journal of Alloys and Compounds,* **404-406**, 2005, pg. 427-430
29. J. Kostka, W. Lohstroh, M. Fichtner, H. Hahn, *Journal of Physical Chemistry C,* **111**, pg. 14026-14029
30. U. Bosenberg, S. Doppiu, L. Mosegaard, G. Barkhordarian, N. Eigen, A. Borgschulte, T. Jensen, Y Cerenius, O. Gutfleisch, T. Klassen, N. Dornheim, R. Bormann, *Acta Materialia,* **55**, 2007, pg. 3951-3958
31. S. Orimo, Y. Nakmori, N. Ohba, K. Miwa, M. Aoki, S. Towata, A. Zuttel, *Applied Physics Letters,* **89**, 2006, pg 21920